SEAFLOOR PRESSURE CHANGE AND ANALYSIS OF ITS EFFECT IN MAJOR EARTHQUAKES OVER JAPAN

JAPONYA BOLGESİNDE DENİZ TABANI BASINÇ DEĞİŞİMİ VE BÜYÜK DEPREMLERE ETKİSİNİN ANALİZİ

SEYEDEH NASRIN GHAFFARI SAEI

ASSIST. PROF. DR. MURAT DURMAZ

Supervisor

PROF. DR. ÇETİN MEKİK (BEÜ)

Co-Supervisor

Submitted to

Graduate School of Science and Engineering of Hacettepe University

as a Partial Fulfilment to the Requirements

for the Award of the Degree of Master of Science

in Geomatics Engineering.

2022

To My Mother...

ABSTRACT

SEAFLOOR PRESSURE CHANGE AND ANALYSIS OF ITS EFFECT IN MAJOR EARTHQUAKES OVER JAPAN

Seyedeh Nasrin GHAFFARI SAEI

Master of Science, Geomatics Engineering
Supervisor: Assist. Prof. Dr. Murat DURMAZ
Co-Supervisor: Prof. Dr. Çetin MEKİK (BEÜ)

January 2022, 84 pages

Pressure changes on the ocean floor may have a relationship with earthquakes that occur around the world. New satellite missions such as the GRACE satellite are able to provide invaluable information about ocean circulations and pressure changes on the seafloor. This study aims to investigate potential relationships between seafloor pressure changes and major earthquakes in Japan. Japan is selected due to its high tectonic activity. The seafloor pressure change time series are obtained from the GRACE satellite and compared with a time series of major earthquakes over Japan during 2002 and 2019. In the analysis, continuous wavelet transforms and wavelet-coherence methods are used. The cross-wavelet transform and phase coherence analysis are applied to determine the correlation between them. The results show that there may be a relationship between seafloor pressure change time series obtained by GRACE satellite and major earthquakes especially between 2011 and 2012. This indicates that seafloor pressure data from GRACE may be used as additional data to study the relationship between major earthquakes and seafloor pressure changes.

Keywords: seafloor, satellite missions, GRACE, hydrography, earthquakes, cross-wavelet transform.

ÖZET

JAPONYA BOLGESİNDE DENİZ TABANI BASINÇ DEĞİŞİMİ VE BÜYÜK DEPREMLERE ETKİSİNİN ANALİZİ

Seyedeh Nasrin GHAFFARI SAEI

Yüksek Lisans, Geomatik Mühendisliği Bölümü
Tez Danışmanı: Dr. Öğr. Üyesi Murat DURMAZ
Eş Danışman: Prof. Dr. Çetin MEKİK (BEÜ)

Ocak 2022, 84 sayfa

Okyanus tabanındaki basınç değişikliklerinin dünya çapında meydana gelen depremlerle ilişkisi olabilir. GRACE uydusu gibi yeni uydu görevleri, okyanus sirkülasyonu ve deniz tabanındaki basınç değişiklikleri hakkında önemli bilgiler sağlayabilmektedir. Bu çalışma deniz tabanı basınç değişiklikleri ile Japonya'daki büyük depremler arasındaki potansiyel ilişkileri araştırmayı amaçlamaktadır. Japonya, yüksek tektonik aktivitesi nedeniyle seçilmiştir. GRACE uydusundan elde edilen deniz tabanı basınç değişimi zaman serileri, 2002 ve 2019 yıllarında Japonya'da meydana gelen büyük depremlerin zaman serisi ile karşılaştırılmıştır. Analizde sürekli dalgacık dönüşümü ve dalgacık-tutarlılık yöntemi kullanılmıştır. Zaman serileri aralarındaki korelasyonu belirlemek için çapraz dalgacık dönüşümü ve faz tutarlılık analizi uygulanmıştır. Analiz sonuçları GRACE uydusu tarafından elde edilen basınç değişimi zaman serileri ile 2011 ve 2012 arasındaki büyük depremler arasında deniz tabanı basınç değişimi arasında bir ilişki olabileceğini göstermektedir. Çalışma ile elde edilen sonuçlar GRACE uydusu ile toplanan verilerinin deniz tabanı basinç değişimi ile büyük depremler arasındaki ilişkiyi incelemek için ek bir veri olarak kullanılabileceğini göstermektedir.

Anahtar kelimeler: deniz tabanı, uydu misyonları, GRACE, hidrografi, depremler, çapraz dalgacık dönüşümü.

ACKNOWLEDGEMENTS

I would like to express my special thanks of gratitude to my supervisor, Assist. Prof. Dr. Murat Durmaz, who has provided me with his knowledge and support throughout my work.

I would like to thank my co-supervisor, Prof. Dr. Çetin Mekik who gave me a golden opportunity to work on this thesis and support throughout my work. I would like to extend my sincere thanks to Prof. Dr. Şenol Hakan Kutoğlu for their insightful comments and suggestions. I would like to express my sincere thanks to Prof. Dr. Ali Özgün Ok, for providing all facilities in the university without which it would not have been possible to complete this study. I would like to thank my jury members Prof. Dr. Şenol Hakan Kutoğlu, Prof. Dr. Ömer Yıldırım, Assoc. Prof. Dr. Saygın Abdikan, Assoc. Prof. Dr. Kamil TEKE for their suggestions and comments.

I would like to thank my family, my mother Zahra Ghassab Nezami, my father SeyedAli Ghaffari Saei, my sister SeyedehShirin Ghaffari Saei and my brother Seyed Mohammad Ghaffari Saei, for always motivating me and making me feel their love.

I would like to thank Şeyhmus Demırkısan, who is always by my side, whose love I always felt, and who I know will always be by my side.

CONTENTS

LIST OF FIGURES

LIST OF TABLES

1 INTRODUCTION

This study aims to analyze the effect of seafloor pressure on the data of GRACE satellite changes by large earthquakes. State-of-the-art methods such as continuous wavelet transform and cross-wavelet transform are explored for analyzing the time series for seafloor pressure changes and earthquakes. This chapter provides a problem explanation with a review of the latest studies on seafloor pressure changes and the use of the wavelet transform. The motivation of the study and its objectives are also listed, along with an outline of the dissertation.

1.1 Motivation

Earthquakes are among the geological hazards in terms of human and financial losses. The main reason for the high human losses is due to earthquakes, where the problem is the lack of knowledge about the time of their occurrence. Therefore, earthquake prediction has attracted the attention of the scientific community in recent decades. Any parameter that changes prior to the occurrence of an earthquake can be a candidate predictor if carefully studied. These may include distortion of the earth's crust, changes in sea level, magnetic and geoelectric earth foreshocks, fluctuations in the earth's gravity field, frequent aftershocks, radon emissions, changes in groundwater levels, animal behavior, and gravimetry.

A lot of research has been done on how earthquakes occur, and the main goal is to reach a point where they can be predicted. In the study of earthquakes, the study of the gravitational field may reveal the deformation of the earth or the ocean floor. While geodetic methods such as (GPS, InSAR) can only detect deformation on the ground and land. By studying variations in the gravitational field, the interactions triggered by an

earthquake can be observed on the ground, so that the mechanism of the earthquake can be better understood.

In 1791, the Chinese were able to predict the Cheng earthquake due to the seismicity rising of aftershocks and animal restlessness and evacuated a large area. Earth's gravity reflects Earth's internal and external mass balance, which includes redistribution of mass owning to ocean currents, tectonics, earthquakes, and ice melt. Therefore, Earth's gravity is a significant parameter in understanding the Earth's dynamics. Geoid, the potential levels in the Earth's gravity field, which is used in the middle of the deep ocean as a mentioned area for all topographic features. Accurate modeling of the Earth's gravitational field is a goal of geodesy. Due to the uniform coverage of the entire world, the Earth's gravitational field is modeled using gravimetric satellites. The Global Positioning System (GPS) provides continuous tracking of satellite orbits, and satellite accelerometers measure non-gravitational forces, including air currents and solar radiation pressure. The CHAMP, GRACE, and GOCE missions opened a new horizon for the study of Earth and its liquid envelope in the areas of ocean dynamics and heat flow, ice sheet equilibrium, crust, hydrology, geodesy, and geophysics [1].

One of the main goals is to explain the principles of specific satellite missions in order to measure the Earth's gravity. GRACE satellite mission monitors gravity changes each month and on a global scale with great and unique precision by pursuing and chasing the variations in the distance between two satellites and combining these dimensions by receiving datasets from onboard accelerometers and GPS measurements. This means that seafloor pressure changes that can be obtained by the GRACE satellites could have epochal implications for earthquakes through the use of the wavelet transform.

The Sumatra-Andaman earthquake with a magnitude of 9.3 Mw occurred on 26 December 2004 at 00:00:53, was one of the toughest earthquakes verified in 40 years [2]. The event on the west coast of North Sumatra occurred after two continental plates shifted along a massive fault beneath the seafloor. The seismic activity triggered tsunami waves that killed an enormous number of people and changed the geography of the Sumatra-Andaman area where islands rose about 20 meters. After that, several researchers and scientists began to explore the probability of utilizing data from GRACE to perceive seismic effects and discover the impact of geodynamic phenomena during an earthquake. Using the numerical model of the tsunami, Bao in 2005 found that the tsunami triggered by the Sumatra-Andaman earthquake could be detected within the measurement range of two GRACE satellites [3]. And the seafloor pressure variances in the Mediterranean Ridge accretionary derived from the GRACE and GRACE-FO satellite missions are investigated which variances appear to link to a rising trend and periods in earthquakes' power time series [55]. The seismically effects of the December 2004 and March 2005 Sumatra earthquakes in the GRACE satellite gravity were used as a wavelet transform. A wavelet analysis helps to find earthquake signatures on the satellite GRACE. A wavelet analysis of the GRACE satellite can be used to detect the geoid deviations triggered by the December 2004 (Mw = 9.2) and March 2005 (Mw = 8.7) Sumatra earthquakes. Two characteristics of time scales for the reduction were found, with a rapid change happening near the central Andaman Ridge. Seismic observations related to crustal and upper mantle density variations and perpendicular movements were discussed in the Andaman Sea [4].

Previous studies of the Sumatra-Andaman earthquake have established the potential of data from GRACE for detecting seismic gravity variations associated with the February 27, 2010, 8.8 magnitude earthquake in Maule, Chile. The earthquakes that happened in

Chile were studied where the variation of sunspot numbers was compared with earthquakes. The studies of solar activity and most significant earthquakes in Chile were performed using the cross-wavelet transform and phase coherence for the sequences of sunspots and earthquake movement, detecting the 8- to 12-year modulation of earthquakes [5]. The possible relationship between sunspot number (SSN) and mean annual precipitation (MAP) in Iran was inspected. Cross-wavelet transform was used to explore the time-based association between the cycles of SSN and MAP. The outcomes of this study indicated that there might be a remarkable correlation among the two-time series of SSN and MAP [6].

1.2 Objective

The main goal of this work is to study the relationship of seafloor pressure changes observed by the GRACE satellite during large earthquakes by investigating state-of-the-art methods such as the continuous and cross-wavelet transforms. To reach this goal, the following objectives are set:

- We require time series of seafloor pressure changes obtained from GRACE satellites from 2002 to 2019.
- Models to verify the time series of seafloor pressure changes are investigated.
- The earthquake-prone region is selected.
- Time series of earthquakes occurring in the selected region from 2002 to 2019 are required.
- Analysis of individual time series and highlight relationships between time series.

1.3 Methodology

The methodology can be summarized as:

- Downloading data from the GRACE satellites from 2002 to 2019.
- Downloading the earthquake data in Japan between 2002 and 2019.
- Extracting time series on seafloor pressure changes from GRACE satellite.
- Extracting time series on earthquakes between 2002 and 2019.
- Applying the continuous wavelet to the time series of seafloor pressure changes.
- Applying the continuous wavelet to the time series of earthquakes.
- Applying the cross-wavelet transform to highlight the relationship between two-time series.
- Analyzing the cross-wavelet transform using the phase coherence.
- Stating conclusions and recommendations for future work.

1.4 Outline

Chapter 1 sets out the motivation, aims, methodology, and outline. Chapter 2 provides theoretical information on satellite missions, their objectives, and their relationships to hydrography, seafloor pressure, earth structure, and earthquakes, and finally provides an introduction to the time series analysis with wavelet transform. Chapter 3, Methodology, describes the general workflow of the data processing, the extraction of the time series, the application of the continuous wavelet transform, the application of the cross-wavelet transform, the analysis of the cross-wavelet transform, and the validation of the data. Chapter 4, Results, represents the results of the study. And finally, Chapter 5, Conclusion, reveals the summary of the study.

2 THORETICAL INFORMATION

Prediction of large earthquakes has become one of the main concerns for current days and it needs a necessity to deal with more effective methods than the traditional ones. Based on the grounds that the pressure changes in the seafloor might provide information about the occurrence of earthquakes and the data could be obtained from the satellite missions, it can provide more comprehensive information about the position of the earthquake, the amount of damage, and its consequences in crowded centers. This information is relayed on the set of operational guidelines from the National Earthquake Information Center to make the best decisions about search and rescue operations.

As a result, satellite imagery revealing new information from each earthquake and putting that information together could provide a possibility to find the impact of the earthquake on the target area. This information, in turn, helps for the estimation of financial facilities and damages, which are critical in the days and weeks following an earthquake. Earthquake effects are currently estimated using seismometers installed on the ground that measure the activity of all vibrations around the earth, but these instruments cannot be placed everywhere on the earth. For this reason, precise data cannot be obtained immediately after an earthquake, and some earthquakes are even more complex and could not be measured with a seismometer alone.

Meanwhile, seismologists have turned to the geodesy to study earthquakes. This science is a branch of applied mathematics that measures and plots the shape and dimensions of the Earth. This method uses satellites and other instruments to complete the information sent by a seismometer. After studying each of the satellites CHAMP, GRACE, and GOCE individually, their characteristics and consumption were analyzed and conclusions were drawn. It is analyzed that the GRACE satellites are suitable for logically detecting ocean pressure changes. This is because their data have great value in deeper areas such as the oceans. To achieve a better understanding of the relationships between the satellites and

hydrography, all the cases and their characteristics and their measurement are studied, through which the changes in pressure on the seabed may well be a precursor for the earthquakes. The movement of tectonic plates causes earthquakes. In addition, to move tectonic plates and alter the mass distribution within the Earth, the effects of earthquakes can cause other mass changes on the Earth's surface, including mass changes in the oceans. The GRACE satellite will be capable of defining the Earth's gravitational field (EGF) at specific time intervals. With the GRACE satellite in orbit, many attempts have been made to determine the deformations caused by large earthquakes using satellite data. Accordingly, the wavelet is a practical tool for filtering local signals and can be used to study the effects of local and temporal changes in the gravity field. Wavelet analysis was applied to gravity signals as well as obtained from gravimetric GRACE satellite observations. In addition to the time series analysis, the gravimetric GRACE satellite observations are utilized to evaluate the time series of data associated with the earthquake. It is worth remarking that both time series are non-stationary, which requires the implementation of the continuous wavelet transform. The cross-wavelet transform (XWT) is then used to study the relationship between the two-time series.

This chapter provides the necessary information to form the theoretical background of the study. Information about different satellite missions provides invaluable information on the gravity field of Earth, ocean currents, and hydrological parameters. Hydrology, ocean bottom pressure, the structure of Earth, and their relationships with earthquakes are also discussed. Finally, background information on frequency domain time series analysis with wavelet transform is given.

2.1 Satellite Missions

Precise determination of the EGF is a necessity for sciences such as geodesy and geophysics. Better information about the EGF leads to more accurate boundary data for studies of the Earth's internal structure. In geodesy, it is vital to have an accurate geoid as a base surface for height determination, which necessitates modeling of the EGF. Ground-based and airborne gravimetric methods for determining the EGF do not have global coverage. In contrast, satellite-based methods have global coverage, although they have lower resolution than ground and air-based methods. Because of the continuous measurements of spatial methods, they can be used to study variations in EGF.

With the launch of newer gravimetric satellites such as CHAMP, GRACE, and GOCE, gravimetry has changed greatly. Currently, a lot of research is being done to use and process the information from these satellites to reconstruct the EGF. These satellites collect a large number of observations during their missions, which must be processed to eventually determine the EGF on a local or global scale. Therefore, in all space missions, the determination of the satellite orbit is one of the most crucial components. For example, determining the position of the system's satellites in space is the basic requirement for the usage of global navigation satellite systems.

Also, for altimetry satellites, it is significant to know the exact position. As the last example, gravity satellites can also be considered. To study the EGF, it is significant to determine the exact position of the satellite. Early space missions used their force models to find out the satellite's orbit and then used astronomical observations to examine the satellite's deviation from its nominal orbit. However, with the advent of the GNSS, the orbit issue has changed dramatically.

Due to the advantages of using GNSS receivers to determine the position of satellites that are at a lower altitude than GNSS satellites, the orbit determination issue has fundamentally changed. Despite the increasing use of GPS receivers in low altitude

satellites, the turning point is the use and installation of the GPS receiver on the TOPEX / POSEIDON satellite in 1992. Specifying a radius below are some of the major projects for low altitude satellites [7].

2.1.1 TOPEX/POSEIDON

It was a joint French-American mission, designed and carried out specifically for oceanography. The satellite's system was launched on August 10, 1992, and had an operational life of at least three years, gradually increasing to more than ten years. The mission was to measure the topography of the oceans using an altimeter.

This type of sensor, the first dual-frequency altimeter, was designed to reduce the error caused by the action of free electrons (known as the ionospheric effect) and provided an altitude measurement with an accuracy of 2.-2.5 (cm). In addition to the altimeter, the mission is also used as a reflector of the SLR system, a DORIS receiver, and a GPS receiver shown at its location [8].

Figure 2.1 TOPEX/POSEIDON Satellite [9].

2.1.2 CHAMP

It was a German mission launched on July 15, 2000. The satellite's mission was scheduled for the last five years, with information available until the end of 2008. One of the main tasks of CHAMP is to determine the EGF with exceptional precision. To do this, it uses the observations of the GPS receivers and the accelerometers for the non-stable forces attached to its body. In addition to these sensors, the satellite carries the reflector of the SLR system to define the position and attitude of the satellite, more precisely the position of the satellite coordinate system, which was relative to the inertial system, and magnetometers to study the magnetospheric layer.

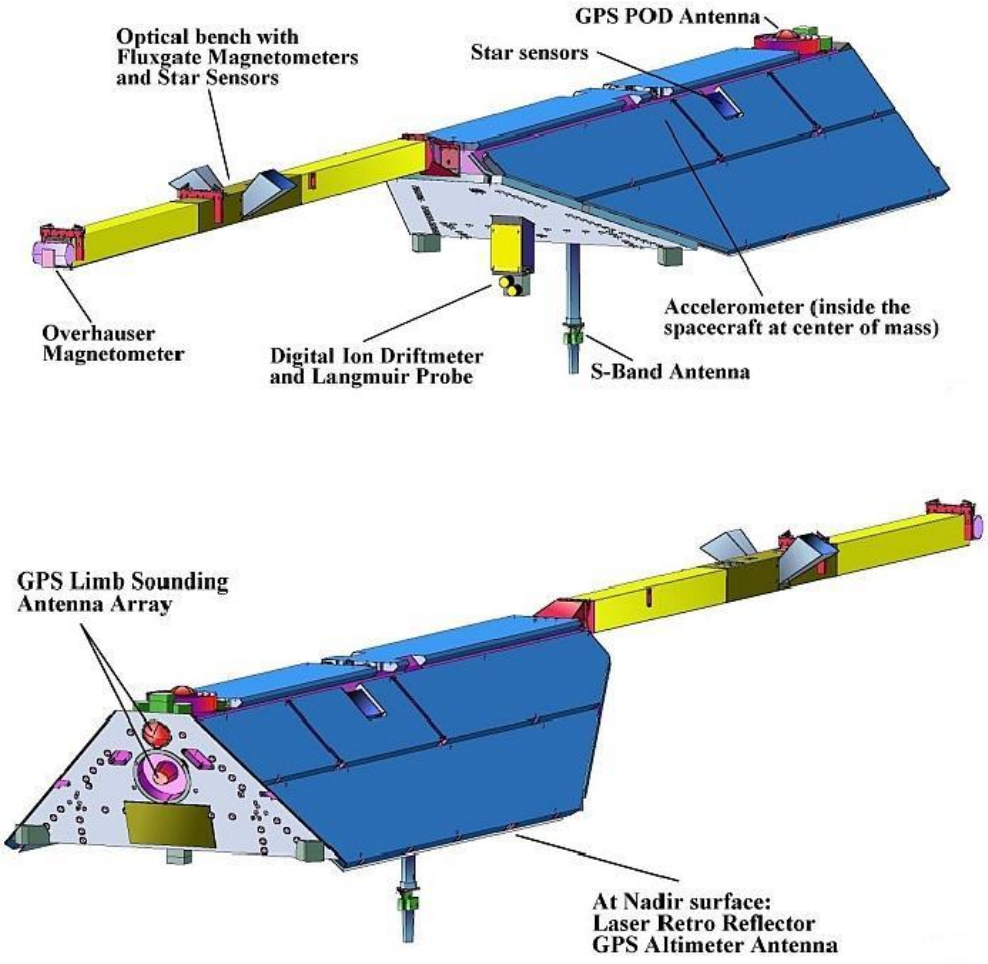

Figure 2.2 Both sides of The CHAMP [10].

The CHAMP was launched from the Russian station Plesetsk on a nearly circular and polar orbit with an initial altitude of 454 km above the Earth's surface and an inclination of 87 degrees. The initial altitude was chosen to best meet the various objectives of the mission. It also guarantees that the system will remain operational for several years, as the altitude is constantly decreasing due to atmospheric friction. On the other hand, this altitude offers a good opportunity to detect the EGF, and the effects which can be seen in

the orbital perturbations of this satellite, and contrastingly, it is suitable for studying the Earth's magnetic field [11].

2.1.3 GRACE

This is a combined mission of Germany and the United States that can be considered a continuation of the CHAMP mission. It was launched on March 17, 2002, at a preliminary altitude of 220 kilometers above Earth orbit. One of its most significant goals is to earn the time-based changes in the EGF with the help of a KBR length measurement system, GPS receiver measurements, and continuous accelerometers. Both satellites are also equipped with SLR and Star Cameras system reflectors.

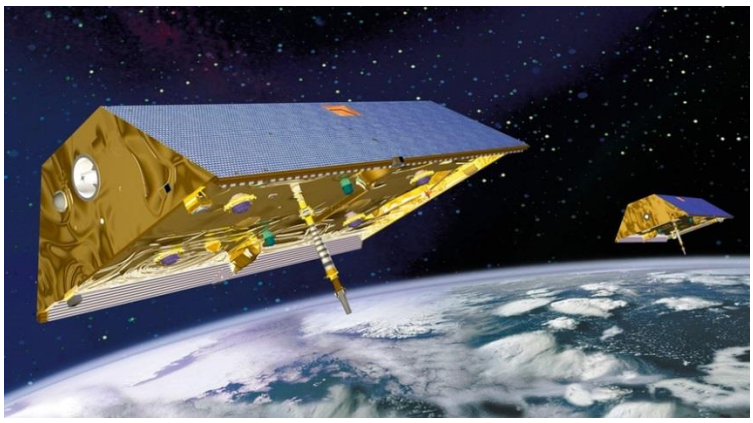

Figure 2.3 The GRACE Satellite Mission. (Image credit: NASA)

GRACE was launched from the Russian station Plesetsk in a nearly circular and polar orbit with a primary altitude of 500 km and a desire of 89 degrees. This mission, like its counterpart (CHAMP), has common characteristics and global coverage. The distance between the satellites of this system is always under control, which constantly fluctuates

in the range of 170-270 Km, and this is done with the help of propulsion, almost all 50 times per day [12].

2.1.4 GOCE

This mission can be considered as complement to the CHAMP and GRACE missions. The satellite was launched on March 17, 2009. The main object of this mission is to determine the static part of the EGF and determine the high precision geoid using continuous gravimeter observations and the GPS receiver installed on this satellite. The satellite is also equipped with SLR and Star Camera System reflectors.

Figure 2.4 GOCE satellite mission [13]

GOCE performs its mission in two parts, with an almost circular orbit of 96.5 degrees and an initial altitude of 250 kilometers, according to the plan. It decreases to 250 km in

the first half and 240 km in the second part. The satellite's very low altitude makes it possible to determine the EGF to the nearest mGal (on average) and to determine a 2 cm precision geoid. (Both of these quantities cause changes in related sciences.) Also, due to the low height of this satellite, it is equipped with a unique and modern electronic propulsion system to deal with the effect of atmospheric friction. The propulsion system continuously adjusts to the effect of atmospheric friction. In other words, this propulsion creates a situation free of friction [14].

2.1.5 Achievements Obtained

With the presentation of the GOCE satellite in 2009, all three satellite missions, CHAMP, GRACE, and GOCE, have reached operational readiness. Information on EGF and its time-based variations have improved dramatically since these missions. At the lower degrees of the EGF, the accuracy of the GRACE satellite model is higher than that of the other models, and in the mid-frequency range from 80 to 140 degrees, the GRACE and GOCE models have the same accuracy. The GOCE model shows its superiority over the GRACE model at short wavelengths of gravity.

Finally, these models are compared with a combined geopotential model in the locating domain, and the accuracy and spatial resolution of each model are measured in this direction. Resolving the EGF and hence, the geoid is one of the fundamental goals of geodesy, but knowledge in this area was inadequate before the use of spatial data.

One of the first achievements in this field was the determination of the degree of flattening of the Earth from the orbital observations of the first satellites. After estimating the flattening of the Earth, limited spherical harmonic coefficients were calculated by using satellite orbit observations. Before the launch of the world's first high-altitude satellite models, the Earth's geopotential models were determined using gravimetric data and

satellite tracking data from ground stations. Geometric grounding and low frequencies of the EGF were determined from satellite tracking observations [15].

It should be prominent that only low degree coefficients of up to 20 could be estimated from satellite observations since there is no uniform and global coverage by terrestrial measuring stations. Determination of the EGF with high precision and dimensional resolution is possible with these observations. These limitations and problems led to the exploration of new observational techniques in addition to satellite-based tracking methods from ground stations.

With the launch of the first altimeter satellite in 1973, the accuracy of gravity field determination increased dramatically in oceanic regions, but in continental regions, the desired and ideal accuracy has not yet been achieved using terrestrial gravimetric data and satellite tracking observations from ground stations. Therefore, the development and application of new spatial observation techniques in continental regions have been more focused on and studied. The results of these studies have been proposed in the form of two general techniques for implementation in specific missions to the EGF:

- Satellite Tracking System (SST)
- Satellite Gradiometer

In a short time, great progress has been made in detecting the EGF using these techniques. These techniques were used in the three satellite missions CHAMP, GRACE, and GOCE. The main features of these three missions are the low polar orbit, the continuous tracking of these satellites in three dimensions using the GPS, and the ability of these satellites to separate the non-gravitational part of the signal from the gravitational signal using accelerometers. For further improvement of the gravity signal, two low altitude satellite tracking techniques were used in the GRACE mission and the gradiometric technique was used in the GOCE mission [16].

2.1.6 Evaluation of the Missions

In order to compare the geopotential models of these satellites, the difference between these models is used and the global models of the EGF in the two domains of frequency and location. For this purpose, three specific models of satellites are utilized:

- AIUB-CHAMP03S
- ITG-GRACE2010S
- GO_CONS_GCF_2_TIM_R3

AIUB-CHAMP03S model from CHAMP satellite to 100 degrees has been calculated using 8 years of observations of this satellite by a celestial mechanical method. The spatial clarity of this model is 200 km [17]. The ITG-GRACE2010S model is available from the GRACE satellite up to 180, corresponding to a three-dimensional resolution of 100 km and using 7 years of data from this satellite [18]. The special GO_CONS_GCF_2_TIM_R3 satellite model is based on GOCE satellite observations from November 2009 to April 2011 up to 250 with a spatial resolution of 80 km by Time-Wise. In this model, the long wavelengths of the EGF are being obtained by using the observations of the kinematic orbit of the satellite, and the short wavelengths are obtained using the Gradiometric observations [19]. Any initial information or geopotential models are available. The EGM2008 model, which is used as a reference to compare the three models is a complete geopotential model up to 2160 degrees with a resolution of 9 km. Satellite altimeter and GRACE satellite geopotential model have been used. It shows the characteristics of each of the missions and the sensitivity of the techniques used in them to a specific frequency range.

It could have pointed to the consideration of the SST-HL technique to long wavelengths and the sensitivity of the SST-LL technique to the average wavelengths of the EGF. One

of the most prominent differences between the models is their low degree of behavior. For grades less than 80, GRACE satellite accuracy is higher than the other two models, indicating that GOCE satellite models are in no way able to compete with GRACE mission models in this frequency range.

The CHAMP satellite is less accurate than the other two models, but the mission-related models have been increased the accuracy and power of the three-dimensional resolution, as well as misaligning the geopotential models that were offered before the satellite gravitational era. In the intermediate frequency range (between 80 and 140), the GRACE and GOCE models exhibit the same behavior. The sudden increase in the difference between the GRACE and GOCE models with the EGM2008 model in this frequency range is due to the use of low-precision ground data in some areas in this hybrid model.

Therefore, it can be specified that the accuracy of GRACE and GOCE models is higher than the EGM2008 model in the middle-frequency range. At short wavelengths of gravity (From 150 degrees and above), the error of the GRACE model gradually increases, while the GOCE model carefully accepts the coefficients associated with this frequency range.

This feature of the GOCE model results from the sensitivity of the Gradiometric technique to the short wavelengths of the EGF and makes the models which are related to this satellite reveal their superiority in this frequency range contrasted to the GRACE mission models. One of the most vital features of special GOCE satellite models is their higher dimensional resolution than the previous CHAMP and GRACE mission models. Comparing the GOCE satellite model with the GRACE model, it should be noted that GOCE is calculated using approximately 1.5 years of data, but the ITG-GRACE2010S model is calculated using 7 years of GRACE satellite data.

In addition to the two assessments made above, comparing GRACE and GOCE satellite models with recent combined geopotential models in the field of space shows interesting

results, especially about the GOCE mission indicating the potential of these missions which is GOCE and EGM2008 are highly compatible in the oceanic areas of Europe, North America, and North Asia. It should be noted that GOCE provides high-resolution geolocation in these areas, which is independent of satellite altimeter data.

In South America, Africa, and the Himalayas, the difference between geoids is at its highest, indicating the low quality and accuracy of the ground data used in these areas in the EGM2008 model. The effect of low-quality Earth data on the altitude geoid is also observed between the latest satellite model, ITG-GRACE2010S, and the EGM 2008 model. However, this effect is much more pronounced with the GOCE satellite model because the short wavelengths of the GRACE model are due to semiconductor fringes and aliasing errors which have lower accuracy. The effect of this inaccurate ground data on the difference in geoid height between the GRACE and GOCE models is not visible. Today, with the launch of the proprietary gravity satellites CHAMP, GRACE, and GOCE, high-accuracy geopolitical models have been created [20].

First, the space features and techniques used in each of these satellites are briefly discussed; then, based on the latest models of specific satellites, geopotential is presented that uses the observations of these satellites to evaluate and compare these missions. The spectral evaluation shows that the satellite model GRACE has higher accuracy at long wavelengths of gravity than the models of the satellites CHAMP and GOCE. At intermediate wavelengths (80 to 140 degrees), the models of the latter two satellites have the same performance and accuracy, and finally, GOCE performs much better than GRACE at short wavelengths.

Thus, by combining the observations from the GRACE and GOCE missions, it is

plausible to obtain geopotential models that have high accuracy in all frequency ranges. Comparison of the quantities computed from these models shows that the GOCE model has a higher dimensional resolution than other models. In addition, one of the most significant results of comparing the models from these satellites with the existing combined geopotential models is the discovery of low-quality observations in some areas in these combined models. This can meaningfully cause identifying weaknesses and improve the existing geopolitical models.

In summary, information on the EGF has been improved expressively after these three satellite missions. The use of monthly GRACE geopotential models is always limited, so their direct use, especially in smaller areas and in applications such as hydrological cycle monitoring, which requires more accurate estimation of the desired signals, poses problems.

Due to the height of the satellite, the potential coefficients of the degree and order in the GRACE geopotential model have low accuracy. Sometimes hydrological models are used to determine the frequency boundary that separates signals from noise. In addition to the absorption target pursued by GRACE satellites, there have been other non-absorption targets. This GRACE satellite mission demonstrates the various modes of mass transfer around the Earth, specifying how much mass is moving and how it changes over time [21].

2.1.7 Rate of Change in Water Storage

Accurate measurements of meteorological parameters such as air pressure, ocean temperature, changes in land water (including soil moisture and groundwater), glaciers, and polar plates, as one of the geophysical components of the fluid, have been challenging. Following changes in meteorological parameters, changes in the EGF due to

changes in mass distribution occur at different time and space scales.

Changes in mass distribution owing to the return of the Earth's solid crust to the pre-glacial period and geophysical processes are responsible in the Earth's core are responsible for producing gravitational field changes in the long run and gravitational field changes at shorter time scales as a result of atmospheric pressures, ocean floor pressures, and surface water storage rates. These short-period changes can be measured by gravitational satellites, including GRACE.

GRACE satellites provide the estimation of the EGF on a regular and monthly basis in the form of geopotential of up to 120 degrees of spherical harmonic coefficients at scales of several hundred kilometers. Compared to terrestrial field measurements such as well drilling, the GRACE satellite mission can be a much more efficient and less costly alternative to examining changes in water storage that have always been difficult on a global scale. The rate of change of water storage is a key parameter for a good comprehension of the hydrological series at local and global scales, and monitoring environmental and climate change. Water storage as a hydrological parameter consists of total precipitation, water evaporation, water runoff from rivers, and infiltration into groundwater. Their accurate measurement can be a valuable constraint for meteorological models and a great help. However, it should be noted that the mass distribution sensed by GRACE satellites includes the sum of all these geophysical sources, and in practice, it is almost impossible to isolate the impact of each of these parameters using its observations. Of course, the results obtained from GRACE can provide a suitable constraint for modeling each of these parameters. In other words; GRACE's main goal is to obtain local information on global water storage changes by recovering changes in the gravitational

field.

Before 2002, there was no global network of observations with the required spatial and temporal resolution so as to show the extent of water storage changes on a continental scale, GRACE's ability to monitor this parameter was very significant. The survival equation related to the amount of water storage variations is:

Increased rainfall - Water evaporation - River water output - penetration into groundwater = Changes in soil moisture + snow cover available at ground level

Measuring and even modeling four factors on the left side of the above equation is considered very difficult. Therefore, in practice, the right side of the above equation, namely soil moisture changes, along with water in snow cover, are used in calculating water storage changes that can be extracted from hydrological models. It is also used to evaluate the output from the GRACE. On the other hand, it has been proven that the overall variation of water storage from the GRACE is from a total of three moisture parameters in the root layer of soil, the water in the snow cover, which can be extracted through global hydrology models, and changes in the surface of the groundwater using measurements of observational wells in the area [22].

2.1.8 Monitoring the Movement of Water

One of the most interesting reasons for the variation of land gravity is the movements of water on the seabed, which has been less interested. By circulating a huge amount of water flow in solid forms, liquid and cavity, inside and above the surface of the earth, with a rapid rate compared to other factors that lead to the place of the land at the ground level, change in the EGF will be created. Therefore, it can be concluded by considering

the changes made in the gravity field, it can be achieved by the amount of mass that changed with the displacement of waters. GRACE satellites measure these changes monthly from 2002.

Today, scientists use numerical models to simulate atmospheric parameters such as rainfall, soil humidity, air temperature, air pressure, and so on. The information provided by GRACE gives us the more realistic output of such models, and by improving these models, it can be promoted correctly to predict weather conditions and changes in the water reserves, managing water resources for domains of agriculture, urban and industrial. Also, under the supervision of water reserves on global scales increases the ability of scientists to predict, plan and respond to unexpected events such as floods and droughts [23].

2.1.9 Icebergs and Global Water Levels

This satellite mission can provide information on the movements of solid water such as polar ice. Once the ice sheets are being melted, the waters absorb a large amount of heat and generate temperature, giving way to reasons the polar ice melting and consequently resulting in a rise in the water level. The fundamental question for the climate is whether the ice sheets are small or large. And whether the water that enters the oceans as the ice sheets melt is constantly raising the sea level. GRACE data has answered these questions and can estimate the number of mass changes that result from melting ice sheets.

A phenomenon called PGR (Post Glacial Rebound), or the slow return of the Earth's crust, to its pre-glacial, where the vertical position of the Earth's crust in altered areas of the

world, including coastlines, creates an error in confirming observations. By combining GRACE data with other satellite data, the contribution of this phenomenon is determined. Altimeter satellites such as TOPEX/POSEIDON and JASON only measure the general changes in sea level. So, by combining the GRACE data with the altimetry satellite data, the issue is the extent to which sea level rise as a result of ice sheet melting is due to the PGR phenomenon or ocean water warming. In other words, GRACE's mass estimate with sea-level rise results from altimetry measurements to separate the estimate of steric and non-steric effects on sea-level change. The volume change indicative of steric changes does not affect gravity changes. Therefore, measurements from the satellite can only detect non-steric effects. Steric effects can be achieved by reducing the observations of variable results at the time of satellite gravimetry. Variable steric signals in time can be used to calculate changes in the amount of heat in the region, and since variable heat storage in the oceans is itself a large source of thermal energy which can predict weather patterns for a long period and occurrence of tornadoes and storms in the future [24].

2.2 Hydrography

Hydrography is defined as "the study, interpretation, and role of oceans, seas, lakes, and rivers." Hydrography has particular importance in dredging operations where there are time and space constraints. Hydrography is used to determine the amount of dredging and to monitor it after dredging. Before, after, and during dredging operations, it is necessary to perform hydrography of the desired area.

Hydrographic maps need to be prepared to assess the amount of layering performed. Performing a hydrographic procedure before and during dredging helps determine the effects of dredging on the marine environment. Hydrography of the discharge area of the

dredged material takes place before the start of the discharge of the material and also regularly and in cycles. Hydrography before dredging is necessary to examine the achievement of the designed goals and its repetition will show the study of shallow levels. Repeated hydrographs and periods help to model the region's sedimentation regime, as well as the economic use of dredgers.

Accuracy and speed are two essential factors in hydrography. The use of modern electronic devices and mini-computer technology has provided new methods for collecting and processing information, the exact position of points where they are measured in-depth, and the level of water at the exact moment automatically with fast distances, with the help of precision devices. Installed on a special hydrographic boat, these devices identify and work on a predetermined area. This information can then be implemented on a map for dredging purposes (planning, reviewing, monitoring) using high-speed printers [25].

2.2.1 Role in Protecting the Environment

Hydrographic data are not limited to the depth and other collected information such as surface position, sound velocity, temperature, sea level (tide), ocean currents, coastal features, shoreline, and seabed material (by sampling or analyzing return signals from the seabed) are measured during hydrographic operations that these data can be used for various purposes. Hydrography plays an essential role in determining marine boundaries and maritime boundaries; because the sea area is defined based on the shoreline (highest mode) and the coastal baselines are generally defined based on the lowest tide, and accordingly, inland waters, local sea, and mainland shelf (up to 200 meters' depth) are defined. On the grounds that most of the marine activities take place in these areas which

need hydrography and accurate charts. Also, from the environmental point of view, these areas are very vital. As a result of the importance of hydrography and the preparation of marine charts, the World Hydrographic Organization was established in 1921 and now has 93 member countries [26].

This organization, while explaining the necessary standards for hydrography and preparation of marine charts, is responsible for the necessary coordination in order to ensure the process of standard hydrography, preparation, and updating of marine charts. Above 70% of the earth's surface is sheltered with water. Today, there is a great talk about mapping other celestial spheres, and space missions are mapping Mars, the moon, etc., while many sea and ocean areas have not yet been hydrographically mapped. This becomes all the more important when it is considered that human life and all living things are dependent on water and that more than 50% of the world's inhabitants live near the coast (up to 50 km). The seas are full of food resources without which life would not be possible; non-living resources, including minerals and oil and gas, provide the energy needed for the industry today. It could be known that climate change on Earth can be affected by the seas and oceans so even small changes in the temperature of seas and ocean currents can lead to widespread environmental changes while disrupting the lives of humans and other living things. In this regard, it can be mentioned global warming, due to the increase in greenhouse gases such as methane and carbon dioxide.

Even though, life is not possible without greenhouse gases (because the earth is so cold and uninhabitable), increasing these gases also raises the earth's temperature and endangers the lives of living things. The seas and oceans play a vital role in absorbing temperature and greenhouse gases and help control the phenomenon of global warming,

but it should be noted that rising the absorption of greenhouse gases by the oceans helps to acidify the water and threatens the life of marine organisms. An example is the destruction of calcium carbonate structures such as coral reefs, which are home to many marine organisms. The information collected by hydrography can help identify the most valuable ecological structures in the seabed while studying the extent of ocean water levels caused by global warming, and provide marine life experts with the extent of its changes [27].

2.2.2 Role in Climate Change

Monitoring sea levels in coastal and offshore areas using coastal alignment stations and satellite data, sea current observations, flow, and tidal modeling is another part of the activities which are carried out by hydrographic organizations and institutions. In this regard, the United Nation's surveying organization has started the development of a permanent network of sea-level monitoring since the 1960s, and now 20 permanent stations are operating on the south and north coasts of the United Nation. This information is used directly in the calculation of datum charts, depth data correction, and preparation of offshore charts.

This information helps seafarers to know the instantaneous depth of water and to sail more confidently on shallow routes such as waterways, access canals, and ponds, so knowing tidal patterns and sea currents can reduce the maritime risk while reducing accidents. In addition, marine current models which is including constant currents and tidal currents, cause marine pollution, such as oil pollution, for moving and spreading in the sea after it has formed can be used to monitor the spread of marine pollution.

Knowing how these pollutants are spread (direction and speed) can be used to deal with them so that they can act more appropriately and more quickly to eliminate these contaminants. The movement of oil slicks to the shores, especially offshore facilities such as desalination plants, can be very risky and disruptive to the flow of life in the towns and villages of the region while imposing high costs on offshore facilities. In such cases, facilities can be identified using current flow models to take the necessary measures to prevent or reduce potential damage. Measuring sea currents using flowmeter equipment is part of hydrographic activities. Hydrography in combination with geodetic sciences can also be used to calculate and study marine geostrophic flows.

For this purpose, today, the mean sea level (MSS) has been calculated using altimeter satellite data such as (TOPEX/POSEIDON, JASON 1 & 2 & 3) and then in combination with the geoid model (obtained by satellite gravimetry). The mean dynamic topography (MDT) is transformed and eventually leads to the speed and direction of sea currents. Sea currents, due to heat transfer (energy), play a very significant role in creating a suitable environment for humans and other living things on the planet, and therefore its changes can cause far-reaching climate change. A look at the numerous projects undertaken worldwide in the study of marine currents confirms the importance of this issue [28].

2.2.3 Role in Tsunami Management

Coastline zones have always been influenced by storms, and tsunamis are possible in seismic areas. Earthquake-induced seismic tsunamis occur on the seabed, and the resulting waves travel rapidly across the sea to the shore. The speed of tsunami waves in deep water is high (up to 800 km per hour), its wavelength is long (up to 200 km) and the wave height is small (up to one meter), which makes it difficult to detect tsunamis in deep

water [29].

As the tsunami approaches the shallow coastal areas, its speed is greatly reduced and the wave height is increased. These high waves (up to several meters) can penetrate for miles on land and destroy coastal industries and human and animal habitats. Large tsunamis can damage coastal facilities and industries and pollute the environment while threatening the lives of humans and other living things in coastal areas. For example, the tsunami triggered by the earthquake on December 26, 2004, in Indonesia with a magnitude of 9.1, killed more than 227,000 people and caused great damage to the countries bordering the Indian Ocean [30].

An earthquake and tsunami in Japan with a magnitude of 9, on March 11, 2011, killed more than 18,000 people and caused the world's largest post-Chernobyl nuclear disaster. Although the Fukushima nuclear power plant was prepared to withstand waves of up to 7.5 meters and the devices were inevitably power cut by the earthquake, tsunami waves entered the plant at a height of 14 meters (up to 15 meters in some reports) 15 minutes after the earthquake. The plant site was completely flooded, and with the power outage and cooling pumps off, the reactors melted and radioactive radiation was affected for miles around the area [31].

The coasts of Iran, especially in the Makran region in southeastern Iran, due to the seismicity of the region and the presence of subsidence, are prone to possible tsunami damage that could endanger the lives of coastal residents and coastal facilities. The speed of tsunami waves and their height depend on the topography of the seabed, and therefore, complete tsunami modeling requires accurate information of the seabed, which is obtained by hydrography. It is obvious that the development of Makran beaches,

regardless of the tsunami risk, can impose many life and environmental effects on the country [32].

Accurate tsunami models can provide suitable locations for the development of the coast as well as the infrastructure of the area to protect the infrastructure of the area from damage in the event of a tsunami. Coastal alignment stations can also record abnormal sea-level changes in the event of a tsunami and send out tsunami warnings.

2.3 Seafloor Pressure and Relations

With the aim of better comprehending the execution of the GRACE satellite in hydrography, it is best to first point out the changes in seafloor pressure and its relationship to major earthquakes as well as the changes in sea pressure, earthquakes, and tsunamis, and how they occur.

2.3.1 Seafloor Pressure

Atmospheric pressure is the weight applied above the atmosphere per unit area which can be measured with a mercury barometer. In most cases, atmospheric pressure is calculated with accurate estimation by hydrostatic pressure. In place of the altitude rises, the atmospheric mass above the reference point decreases, and therefore, as the altitude increases, the atmospheric pressure decreases. As may be well known, pressure is distinct in utilizing the force per unit area, and the unit of pressure in SI is Pascal. As mentioned, atmospheric pressure can be measured with a barometer. This mercury barometer consists of a long glass tube full of mercury that is placed upside down in a container of mercury. When the tube is placed upside down in the container, mercury is transferred from the top of the tube into the container. As a result, a vacuum is created at the top of the pipe. This

is due to the pressure difference between the tube and the container, and when the pressure reaches equilibrium, a height equal to "h" is considered. At this altitude, the pressure exerted on the mercury is equal at two points "E" and "D". Point E pressure is the pressure of the mercury column, while point D pressure is the atmospheric pressure above it [33].

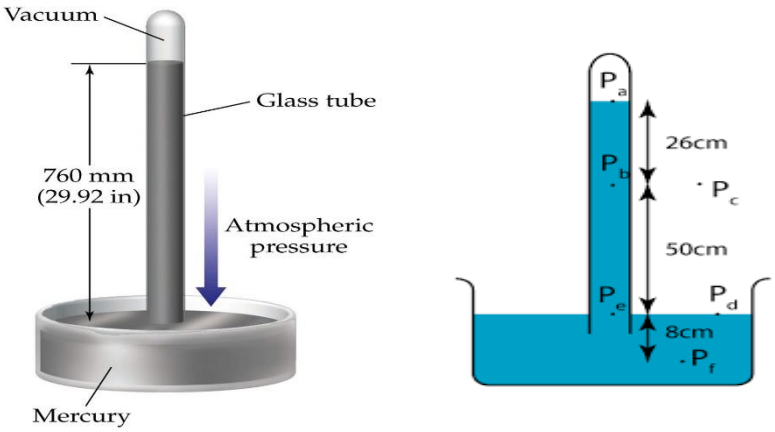

Figure 2.5 Barometer pressure [34].

It could be calculated the pressure of point E using the height h.

$$p = \rho g h \tag{2.1}$$

In the above relation, the density of mercury is equal to 13.6 g / cm3 and the acceleration of gravity is equal to 9.8 m / s squared. The average value of h at sea level is about 76 cm. Therefore, using the above numbers, the atmospheric pressure will be 101,325 Pascal. The pressure on the ground changes with altitude. If it wants to be calculated this value accurately, it must be taken such factors into account. Above sea level, for every 100 meters, the pressure decreases by 1.2 KPa. Atmospheric pressure due to weathering

shows daily cycles (or 2 times a day). This effect is greater in the tropics and close to zero in the polar regions. A pressure of 1 atmosphere (101.325 KPa) is also the pressure exerted by a 3.3 m long water column. It is better to declare about the ocean current and wave power. There is a stream of water in an ocean. Streams are rivers which temperature is lower or higher than the temperature of the ocean. These currents are often in the form of a circle or a complete cycle. One of the most significant and famous sea currents is the Gulf Stream, which transports hot air from one point of the earth to another. The presence of currents in the oceans has been discovered by sailors. In the early 18th century, American merchant ship captains were aware of the existence of the Gulf Stream and its course and used its power when traveling to Europe. The first draft of the Gulf Stream was published in 1770 by Benjamin Franklin. In it, the Gulf Stream is depicted as a wide river flowing in the ocean [35].

2.3.2 Factors Causing Ocean Currents

There are several factors involved in creating currents, but the main one is with prevailing winds. In the realm of dominant winds, the direction of surface currents is the same as the direction of the wind. The impact of currents on shores or underwater ridges changes their course. In addition, ocean currents, like any other moving object on the Earth's surface, are affected by the Coriolis force. In the Arctic Basin, evaporation is extremely low due to extreme cold.

On the other hand, the great rivers of Asia and Europe enter it with a large amount of water, so its level is slightly higher than the general level, and therefore there is a difference in the level of currents that excess water discharging into the Atlantic and Pacific oceans. In the Mediterranean, evaporation is greater than the amount of water that enters it through rivers and rain. As a result, to compensate for this shortage, the waters of the Atlantic flow to the Mediterranean. The hot, salty waters of the Gulf Stream sink

deeper into the colder polar waters as they become heavier. Where two ocean currents meet, the water goes deeper, and conversely, where the two currents move away, the deep water rises to the surface of the ocean [36].

2.3.3 The Structure of the Earth

The ground under our feet looks solid, however, it is in motion. The world consists of three main layers. The crust which is only one percent of the outer layer is made of rock. Under the crust is another layer, the Earth's mantle, which consists of softer, thicker, and more viscous rock and makes up about 3 percent of the Earth's volume. The very hot core of the Earth, which consists of an outer (liquid) and an inner (solid) part, is made of iron and nickel [37].

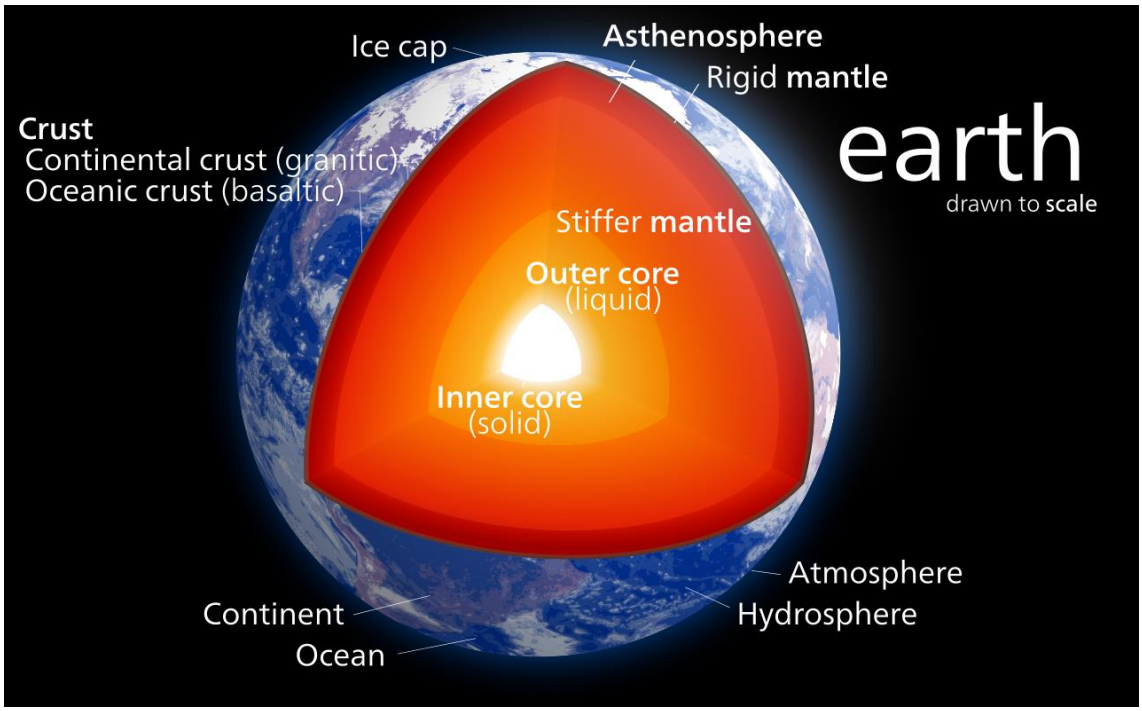

Figure 2.6 Earth's structure [38].

2.3.4 Fault

To get a better idea, consider that the surface of the earth is a plate of hard rock lying on a thick, sticky ocean. These planes move, very slowly, over millions of years. Sometimes they get away from each other, sometimes they get close to each other. Where two or more planes have collided, it is called a fault [39].

2.3.5 Earthquake

When planes move horizontally in two contrary directions or one direction at opposite speeds. Generally, collision happens and one goes below the opposite. Sometimes when two plates collide, one (usually the oceanic crust) does not go under the other, but the pressure of the collision of the two plates appears as a fold in the crust called a mountain. This is the reason why, for example, the height of Mount Everest increases. While two planes move vertically or horizontally in a relative manner, an oversized quantity of energy is produced at the surface of the planet, which is named earthquake. Once this energy exceeds the carrying capacity of the crustal rock at the fault, the fault begins to slide, and damaging energy is discharged [39].

2.3.6 Aftershock

After each earthquake, energy is still released, but its size gradually decreases. These weaker earthquakes are called aftershocks, which are usually smaller than the original earthquake. The aftershocks themselves can be destructive and cause more damage to structures damaged in the main earthquake. The aftershocks may continue for up to two years after the main earthquake. Every earthquake has a geographic point, that is, the main location (epicenter) where the energy is free by an impact or landslide. If the

geographic point of the earthquake is below the ocean, it would cause vast waves called tsunamis. The deeper the epicenter, the weaker the waves reach the surface. The area on the ground above the epicenter is called the epicenter. Identifying the depth of an earthquake is more difficult than identifying the epicenter. To determine the depth of the earthquake, seismic stations should be near it.

Earthquakes are now measured on a large or large scale (MW) worldwide, and the Richter scale is obsolete. The simple reason is that magnitude more accurately measures the magnitude of an earthquake, especially in earthquakes above five, and has therefore replaced Richter. The magnitude of an earthquake is dignified by another unit called the Mercalli. This scale is twelve degrees, up to seven degrees of destruction is negligible. At magnitude eight, weak buildings collapse and there is a lot of destruction from above. Magnitude is not always directly related to the intensity (destructive power) of an earthquake. Earthquake, vibration, and movement of the earth that occurs owing to the release of energy discharged from rocks in faults in the earth's crust in a short time. The place where the earthquake originates and the energy comes out is named the hypocenter, and the focal point above the earth's surface is named the epicenter. Before the main earthquake, relatively mild earthquakes usually occur in the region, known as pre-earthquakes.

Subsequent earthquakes are also called aftershocks, which occur with less intensity and with different time intervals between minutes and months. The greater the number of aftershocks, the smaller the magnitude of the main earthquake. Earthquakes are the outcome of the unexpected release of energy from within the earth's crust that generates vibration waves. Earthquakes are verified with a seismometer or seismograph. The deeper

the epicenter, the less damage there is. The magnitude of a quake is relational to the energy unconfined by the earthquake. Earthquakes smaller than 3 Richter magnitude regularly cause imperceptible damage and magnitude greater than 6 Richter magnitude. Numerous other distances (greater depth of impact less than 10 km to 700 km as well as the greater horizontal distance from the center) to the direction of vibration (vertical or impact) and the type of vibration wavelength [39].

Earthquake waves have three types, P and S (body waves) and surface waves. The first type of P is known as compression or longitudinal waves because its waves are shocked and vibrate in the direction of propagation (such as playing a rope) and in the earth's crust with a velocity of 1. They travel at 5 to 8 kilometers per second, unlike S-waves or shear waves, which are up to 1.7 times slower and vibrate perpendicular to the propagation line (such as shaking a tablecloth) but cannot pass through liquids such as water or molten rock such as the outer core. A strong earthquake at a depth of 105 degrees shakes the surface areas, and the areas beyond this angle are called the shadow region. The direction of passage through the outer mantle or core of the earth shook an area far from the center. Near the earth's surface, earthquakes appear as vibrations or sometimes earthquakes. When the epicenter is in the sea, large and rapid deformation of the seabed causes a tsunami, which usually occurs in earthquakes larger than eight magnitudes. Earthquakes cause mountains to collapse, as well as volcanic activity. Overall, the word earthquake includes any kind of natural or man-made human vibration which reasons vibration waves. Earthquakes are often the result of faulting, but can also be the result of volcanic activity, landslides, mine explosions, and nuclear experiments [40].

2.3.7 The Magnitude of an Earthquake

The magnitude of an earthquake is M equal to the logarithm at the base of the ten amplitude of maximum (in microns) motion, A, recorded by the standard Wood Anderson seismometer 100 km from the epicenter.

$$M = \log 10A \tag{2.2}$$

Also, to determine the energy released by each earthquake, a relation was developed by Richter-Gutenberg in 1956, which specifies the amount of energy released at the epicenter in terms of the organ (erg) which is the unit of the energy and its magnitude "M".

$$\log E = 4.8 + 1.5M \tag{2.3}$$

A simple calculation can be shown that by increasing the magnitude of an earthquake by one degree, the amount of energy released increases approximately 32-fold [41].

2.3.8 Types of Earthquakes

Earthquakes are divided into horizontal and vertical types in terms of energy release. Major and extensive damage is usually caused by horizontal earthquakes, for instance; most buildings have sufficient resistance to vertical loads. According to the amount of damage, earthquakes are divided into twelve degrees based on Mercalli [42].

Understanding, the causes that bring earthquakes makes us achieve useful information about the relationship between the pressure changes that makes this phenomenon and recognize how it could be managed by finding its relation with GRACE satellites.

2.4 Japan

The Japanese archipelago is an island nation in East Asia, sited in the Pacific Northwest. Japan is bordered by Russia to the north and the Sea of Japan, China, North Korea, and South Korea to the west. The 2011 Tohoku earthquake and tsunami with the magnitude 9.0 was an earthquake that occurred at 2:46 p.m. local time on March 11, 2011, near Sendai in northeastern Japan's Miyagi Prefecture for 173 seconds. The epicenter was below the floor of the Pacific Ocean, but no tsunami alert was given out. Tsunami alerts were issued in at least 20 additional seaside areas in South and North America. It caused minor disasters in other countries. On April 1, the Japanese government officially named the disaster the "Great East Japan Earthquake." Before the magnitude 9 earthquake, there were 9 earthquakes in the region, the largest of which, with a magnitude of 7.1 on March 9, can be considered a devastating magnitude 9 earthquake.

More than 18,000 people in the tsunami were killed and the bodies of 2,531 were never found. The quake quickly triggered tsunamis in Japan and 20 other countries along the North and South Pacific, including North America and Chile. In Japan, the highest tsunami alert was issued, and loudspeakers, radio, and television were urged to evacuate near the sea immediately and take refuge in the highlands. The height of the tsunami was 10 meters. The deadly and destructive effects of a tsunami are more countless than those of an earthquake. The post-tsunami images of the city of Miami show that even traces of the city's existence remain. The destruction of the city indicates that the height of the tsunami in this area was more than 10 meters [43].

2.5 Frequency Domain Time Series Analysis

Different methods for the study of the time series have existed. Since Fourier and wavelet

transform analyzes are used in the time series in this study needed only those methods will be discussed here. The wavelet transforms were utilized to better understand the time series of earthquakes in Japan and the time series analysis we created on the GRACE satellite. The wavelet transform (WT) is one of the greatest significant scientific transformations utilized in numerous fields of science. The chief impression of the WT is to overwhelm the weaknesses and limits of the Fourier transform (FT). Contrasting to the FT, this transformation can also be implemented for non-stationary signals and dynamic structures. Mathematical transforms have many applications in processing and classifying various data such as signals and time series. For example, the FT can be utilized to transfer a signal from time to frequency. The peaks in the frequency spectrum of a signal after applying the FT represent the frequencies at which the signal is dominant which is being worthwhile in the case of the sharp and large peaks. The location of the peak (frequency value) and its height (frequency range) in a frequency spectrum graph can be used as input to classification algorithms such as Random Forest or Gradient Boosting [44]. The following sections describe the Fourier and wavelet transforms to understand the time series used in this study.

2.5.1 Fourier Transform

The general rule about the FT is that it performs well as long as the signal is stationary. Stationarity means that the frequencies occurring in a signal are not depending on the time. Processing non-stationary signals are usually more difficult and other techniques and pre-processing must be used to analyze them. Many of the real signals in nature are not stationary.

As it is known, the FT executes by proliferating the processed signal by a sequence of sinusoidal signals with disparate frequencies. If the point multiplication operator between the desired signal and a sinusoidal signal with a definite frequency is equal to a number

with a large amplitude, so it can be concluded that there is a large overlap between these two signals and thus a certain frequency in the frequency range of the desired signal. This is certainly because the multiplier is a standard point for measuring the degree of overlap and similarity between two vectors or two signals.

It can be said about the FT that it has a great resolution in the frequency area. To put it another way, the FT expresses what frequencies are in a signal, but it cannot be used to determine at what time the desired frequency occurs in the signal. Therefore, it is not possible with the FT to know exactly where the frequency occurs in the main signal. To solve this problem, the Short Time Fourier Transform (STFT) method will be used. In this technique, the main signal is divided into numerous sections of equal length. These sections might or might not overlap. The signal is divided into several sections before the FT is performed. The basic clue of this method is very easy. For instance, if the signal is divided into 5 sections and the FT identifies a certain frequency in the third part, it can be said with a high degree of certainty that this frequency is between 3/5 and 4/5 of the main signal.

However, the biggest disadvantage of this method is that the FT is subject to a physical limitation called uncertainty. The smaller the window size, the more accurately it can determine when a frequency occurs from the main signal, but on the other hand, it obtains less information about the frequency value of the main signal. The larger the window size, the more information about the frequency value and the less information about when the frequency occurs. An improved way to analyze a signal with a dynamic frequency spectrum is to use the WT which has a significant resolution in both the time and frequency domain. This transformation determines not only the number of frequencies in the signal, but also when these frequencies occur from the signal. The WT reaches this capability by operating at different scales.

The size and direction of the blocks can be specified the degree of resolution in that conversion, in other words, the blocks in each conversion determine how small the features in that time and frequency domain can be identified with that conversion. The main signal has a great resolution in the time domain, unlike the frequency domain. The STFT has a medium resolution in both the time and frequency domains. The resolution of the WT changes on the grounds that for low or high-frequency values, it has a direct relation with the time and indirect relation with frequency. Therefore, in general, it can be said that the WT is a compromise on scales where time-dependent properties are more attractive.

As mentioned earlier, the FT utilizes a series of sine waves at different frequencies to evaluate the signal. In this case, the signal is represented as a linear combination of sinusoidal signals. The WT, on the other hand, uses several functions termed wavelets, each of which has a different scale. As is known, the word wavelet means small wave, and the wavelet functions are the same.

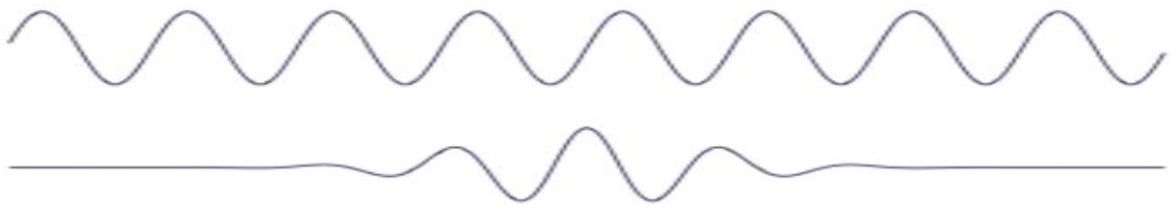

Figure 2.7 Difference between sine signal (first line) and wavelet (second line)

Figure 2.7 is presented that the sinusoidal signal is not at a specific point in time. This signal begins at infinity and continues to infinity while a wavelet is localized at a specific point in time. This property allows the WT to acquire time information in addition to frequency information.

Since the wavelet is located in time, the original signal can be multiplied by the wavelet at different points in time. The first step is to start with the initial points of the signal and transfer the wavelet step by step to the end of the signal. This process is called *convolution*. After convolution with the main wavelet signal (mother wavelet), it can be scaled to a larger size, and the process is repeated. The WT is often expressed in terms of scaling. The most common method of studying the properties of signals that are not unique in the time domain is to compare them with a set of basic functions [44, 45].

2.5.2 Wavelet Transform

Wavelets are the groups of mathematical functions that are continuously utilized as proofs in their frequency parts, with the resolution of every part corresponding to its scale. The WT is that the decomposition of an operates supported moving ridge functions. Wavelets area unit transmitted and scaled samples of an operate (mother wavelet) of finely arched and extremely attenuated length.

Since the time series data is not stationary, it needs to corroborate the data with continuous wavelet transforms (CWT), which must be understood provisionally. The CWT was settled as another STFT to solve the resolution problem. Wavelet analysis is performed like STFT. The signal is reproduced by a function that is analogous to the window function in STFT, and the transformation is calculated distinctly for alternative parts of the signal over time. Though, two vital differences between CWT and STFT have existed:

- FTs window signals are not calculated, and therefore the signal peaks are assumed to be sinusoidal, which means that negative frequencies are not considered.
- The width of the window varies with the calculation of each component of the spectrum, which is probably the most significant property of the WT.

Although the square of time and the frequency resolution measurements act as the results of a natural phenomenon, every signal is analyzed employing a completely different approach which is known as multi-resolution analysis (MRA). MRA analyzes the signal at totally different frequencies with various resolutions [45]. In this case, each component of the spectrum does not decay, as well as being the case with STFT. This approach is particularly useful when the signal has short periods with high-frequency components and longer periods with low-frequency components. The signals we encounter in practical applications are often of this type.

The term wavelet means a small wave. Smallness in this context means that the function (window) has a limited length (compact fuse). The wavelet also means that it is an oscillating function. The term mother means that functions with different positions and backups utilized in the conversion method are resultant from a mother function or a mother wavelet. This formulation refers to temporal information in the conversion space. Unlike the STFT, in this case, the scale parameter is implemented.

The scale in wavelet analysis is analogous to the scale used in maps. As with the map, the upper scales represent a general view without details and the lower scales represent a more detailed view. The situation is similar for frequencies: Low frequencies do not denote the general information of a signal (which usually covers the entire range of a signal), whereas high frequencies do not signify the detailed information of a hidden pattern.

In practical applications, low scales (high frequencies) do not cover the entire signal period and appear explosive over time, while high scales (low frequencies) usually persist over the whole signal period. Scaling is a mathematical operation that can compress or open up a signal. Larger scales represent open signals and smaller scales represent compressed signals. All signals are derived from a similar cosine or sine signal. In other

words, the opened or compressed versions are cosine or sine.

If Y (t) is a mathematical function, then Y (st) is a compressed Y(t) if s > 1, and an open version if s < 1. Though in the explanation of the WT, the scale is utilized in the denominator, i.e., the inverse of the above expression, s > 1 opens the signal, and s < 1 compresses the signal. Assume Y (t) is the signal to be decomposed. The mother wavelet is selected as an original for all windows. All windows utilized are opened and shifted versions of the mother wavelet. Several functions are used for this purpose. After the mother wavelet is selected, calculations begin with s = 1 and the CWT is calculated for all values of s greater than one and less than one. Though, depending on the signal, a full conversion is usually not required. For all practical purposes, the signal is limited. Therefore, the conversion calculation is sufficient for the limited time intervals of the scales.

For simplicity, the process begins with a scale of s = 1 and continues with increasing values of s, meaning that the decomposition begins at high frequencies and continues at low frequencies. The initial value of s represents the most compact wavelet. As the value of s increases, the wavelet opens up. The wavelet is positioned at the beginning of the signal, at the point where time is zero. The wavelet function is multiplied by a scale of the signal and then summed over all products of the multiplications. The result is multiplied by the constant number 1 / sqrt. This multiplication is utilized for energy normalization so that the converted signal has the same energy for all scales. The final result is the conversion value, i.e., the CWT value at time zero of scale s = 1. In other words, this value corresponds to the point $\tau = 0$ and s = 1 on the time scale. The wavelet at the scale s = 1 is then shifted to the right of τ, $t = \tau$, and is calculated to obtain the conversion values at $t = \tau$ and s = 1 in the frequency space.

This method continues until the ripple reaches the tip of the signal. At this point, a row of

time scale points is computed for s = 1. Then, s increases slightly. A reminder that this is a continuous conversion and τ and s must be continuous increase. Now if this process is to be performed by a computer, both of these parameters will increase to a suitable small size. This means sampling on a time scale. The above process is repetitive for all s values [45].

Accordingly, CWT is a transformation that takes a continuous function in time into the space of time-frequency. The foundations of the new house square measure ripple functions. For example, the periodic properties of a signal are studied with an exponential $e^{J}\frac{2\pi}{T}nt$ function. If the base function ψ_t is scaled and shifted to $\psi\,(\frac{t-b}{a})$, the resulting display is then called a time-scale or wavelet transformation. The original idea for WT was rooted in the Haar wavelet [46], but it has been developed today by researchers in geophysics, theoretical physics, and mathematics. Scientists discovered a closed relationship between wavelet and multivariate analysis, which led to a simple solution for calculating the mother wavelet. If the center frequency of the base function $\psi\,(t)$ is ω_0, then the center frequency $\psi\,(\frac{t}{a})$ equals to $(\omega) = \frac{\omega 0}{a}$. Consider the signal s(t), the CWT is defined as follows:

$$CWT(a,b) = \frac{1}{\sqrt{a}}\int s(t)\psi^{*}(\frac{t-b}{a})dt \qquad ,a \neq 0 \qquad (2.4)$$

The basic function ψ_t is named the mother wavelet. The parameter a is also the scale index and the parameter b indicates the time shift. If is concentrated at time zero and ω_0 is as frequency. Then $CWT\,(a, b)$ cause to reflect the signal behavior in the neighborhood $(b, \frac{\omega 0}{a})$. In WT, temporal resolution and frequency are a function of the scale coefficient.

The time resolution of Δt and $\Delta\omega$ for wavelet transformation is respectively $a\Delta$t and $\Delta\frac{\omega}{a}$. The quality factor Q for WT is independent of the scale factor a.

$$Q = \frac{\left(2\left(\frac{\Delta\omega}{a}\right)\right)}{\frac{\omega 0}{a}} = 2\frac{\Delta\omega}{\omega 0} \tag{2.5}$$

The square of the size of the CWT is called a Scalogram.

$$SCAL\ (a,b) = |CWT\ (a,b)|^2 \tag{2.6}$$

If it wants to reconstruct the signal from the WT coefficients, the mother wavelet must follow the following condition:

$$C\psi = \frac{1}{2\pi}\int_{-\infty}^{\infty} \frac{|\,\psi\,(\omega)|^{\,2}}{|\omega| d\omega} < \infty \qquad ,\psi\,(0) = 0 \tag{2.7}$$

In the above relation, $|\psi\,(\omega)|$ is the mother wavelet in FT, and the ψ (0) = 0 condition means that the mother wavelet is intermediate. The signal s(t) can be calculated by converting the inverted wavelet from CWT which is the above condition is the admissibility condition. It's better is brought the inverse of WT:

$$Es = \frac{1}{C\psi}\int_a\int_b CWT\ (a,b)\hat{\psi}\left(t - \frac{b}{a}\right) db\frac{da}{a^2} \tag{2.8}$$

In the above relation, $\psi\hat{}\,(t)$ is the mother wavelet, which is normally selected $\psi\hat{} = \psi\,(t)$. Moreover, the weighted energy of the WT on the time-frequency plane is equal to the signal energy in the time domain:

$$Es = \int |s(t)|2dt = \frac{1}{C\psi}\int_a\int_b |CWT\,(a,b)|2\;db\frac{da}{a^2} \qquad (2.9)$$

3 METHODOLOGY

This section describes the methodology applied to reach the objectives of the study, examining the work steps according to the following process. First of all, by downloading the data from the GRACE Satellite and the earthquakes larger than 6Mw then extracting the times series besides applying the continuous wavelet Transform and Cross-Wavelet Transform through analyzing and finally the validation of the results. The below flow chart shows the work process and related subsections, in which each step is explained in detail.

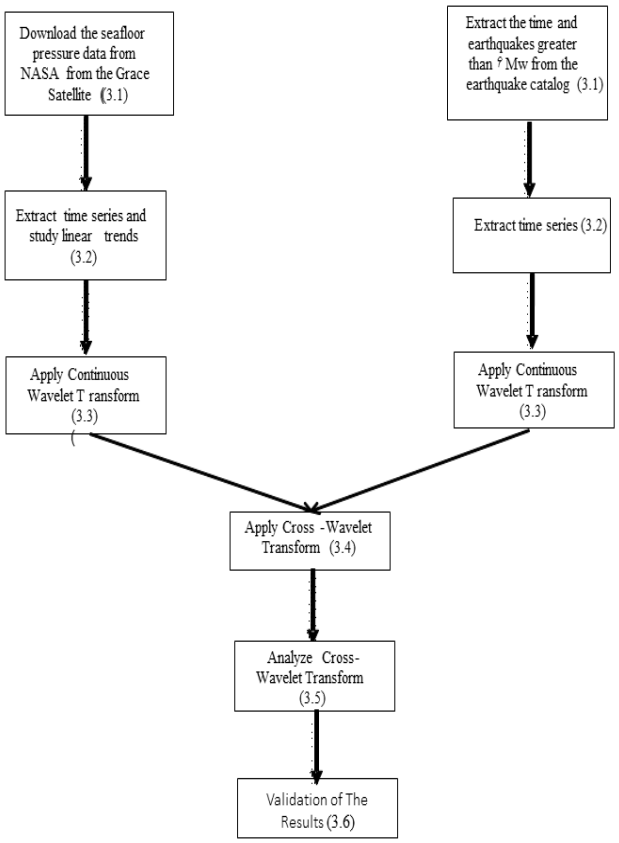

Figure 3.1 General workflow of the study

3.1 Obtaining the Data

In the beginning, the data is downloaded from NASA's site through the GRACE satellite's reports and GRACE-FO (GRACE Follow-on). The data are monthly reports from the GRACE satellite from 2002 to 2019. Each of the data includes a subset of latitude, longitude, time, and equivalent water thickness (LWE). LWE is observed by monthly changes in gravity or mass and is utilized as the seafloor pressure data. The data related to the ocean bottom pressure by the GRACE satellite could be downloaded from the NASA website [47]. A page of data with different formats could be seen in which the NETCDF format is selected which the required items such as seafloor pressure, time, latitude, and longitude are downloaded. It is worth mentioning that in downloading the data, there is a section called Info, by clicking on which all the information related to any data of GRACE satellite can be seen. To better understand the variables, it is possible to read the variables of NETCDF format by using the "ncread" function for every detail that needs to be analyzed. To examine the changes in the data compared to the earthquakes in Japan, earthquakes with a magnitude of more than 6Mw are extracted for 2002 to 2019 years by the Earthquake Catalog in Japan. It is worth mentioning that from 2002 to 2019, every year except 2017, earthquakes of more than 6Mw have occurred in Japan, and for example, in 2005, two earthquakes with the magnitude of 7Mw and 7.2Mw have occurred. In this case, the average of these earthquakes is considered.

3.1.1 Selecting the Region

GRACE satellite data gives us seafloor pressure on a temporal basis, the data are also based on latitude and longitude in monthly time intervals by averaging the seafloor pressure changes. Japan's range is specified by latitude and longitude from the extraction of seafloor pressure changes. The seafloor pressure time series is averaged over several latitudes and longitudes around Japan. An example is given from the left of the first column latitude, second column longitude, and third column LWE at the time of the first

month of 2010.

21 131 1.5

21 132 2.5

21 133 2.6

21 133 2.2

The average of the third column is for the first month of 2010.

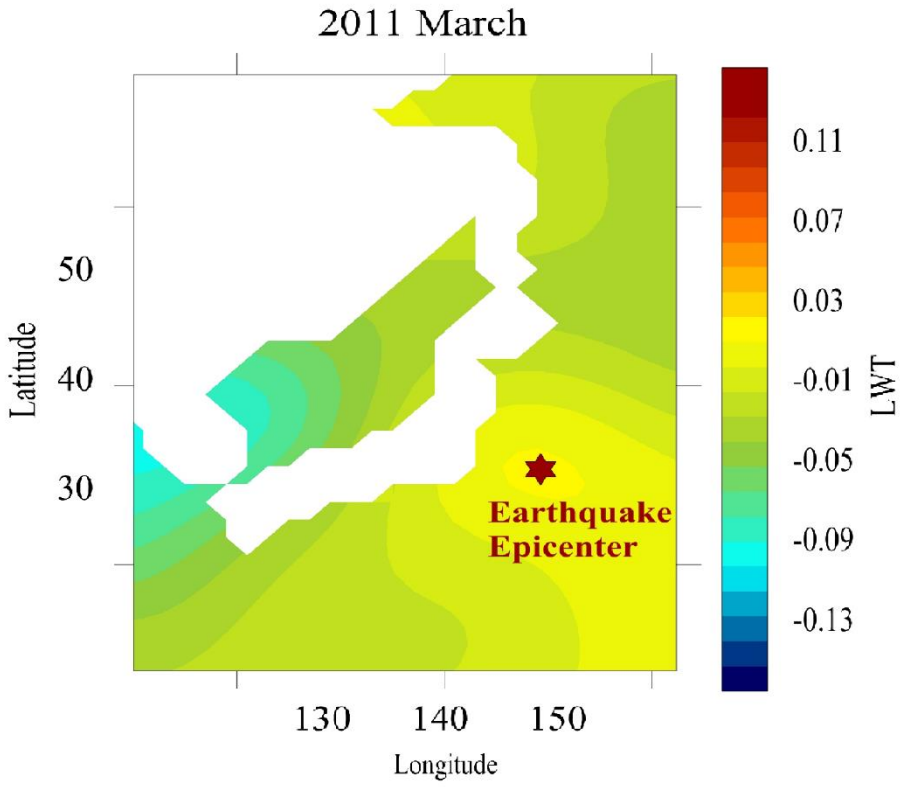

Figure 3.2 The averaging area in Japan

Figure 3.2 illustrates the seafloor pressure distributions around Japan through 2011 in which the white areas are lands, and the seafloor pressure changes are zero or near zero in those areas. It is better to express that the seafloor pressure has the same range of the fault line, and in other ranges, the seafloor pressure is zero, there is no need to extract the

seafloor pressure only at the fault lines, and the fault lines are not complete, they are just recorded based on the earthquakes that have been occurred and through the existing maps [48].

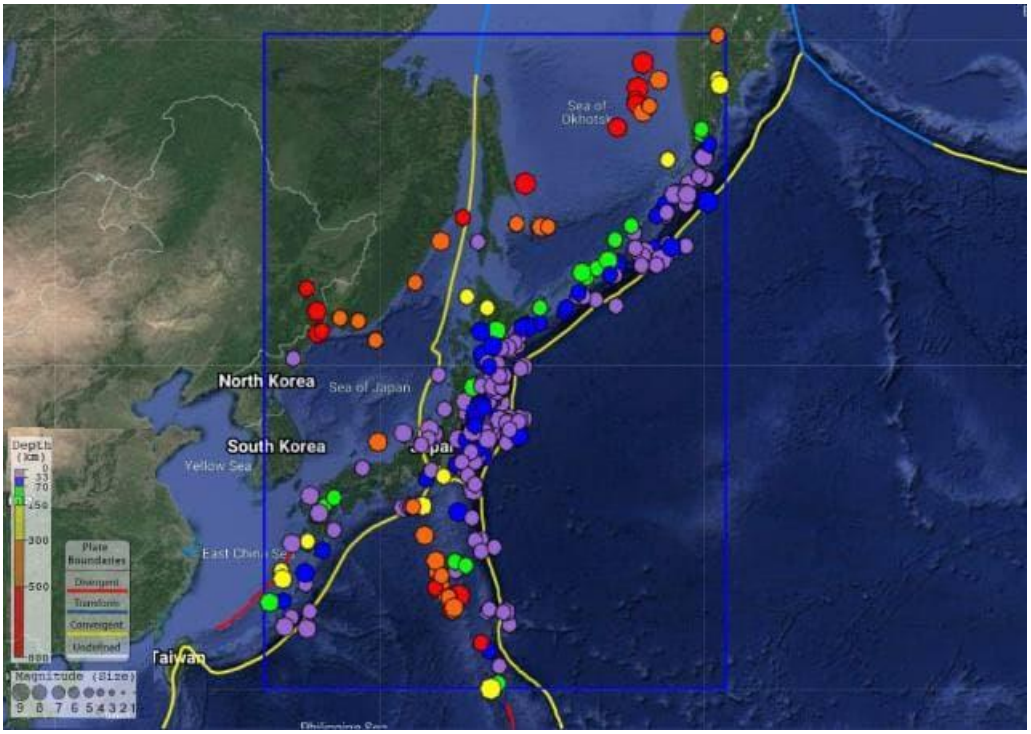

Figure 3.3 Earthquakes that Happened in Japan between 2002 and 2019 [49]

Japan's earthquakes occur mostly in the ocean because the oceanic plate goes under the land surface. Figure 3.3 presents the earthquakes that occurred in Japan which are significant in the case of study and declares that earthquakes generally happened on the coastline and oceanic surfaces.

3.2 Extracting Time Series

In this step, a series of times for the seafloor pressure data is created, and then because

there are gaps in the dataset, the interpolation in the MATLAB environment is performed, and all the steps such as linear, cubic, spline, nearest are done to construct the new points in a discrete set of data points. The datasets that are being as gaps could see in the following table which makes the time series interpolate datasets which the gaps in datasets are settled by the NASA website.

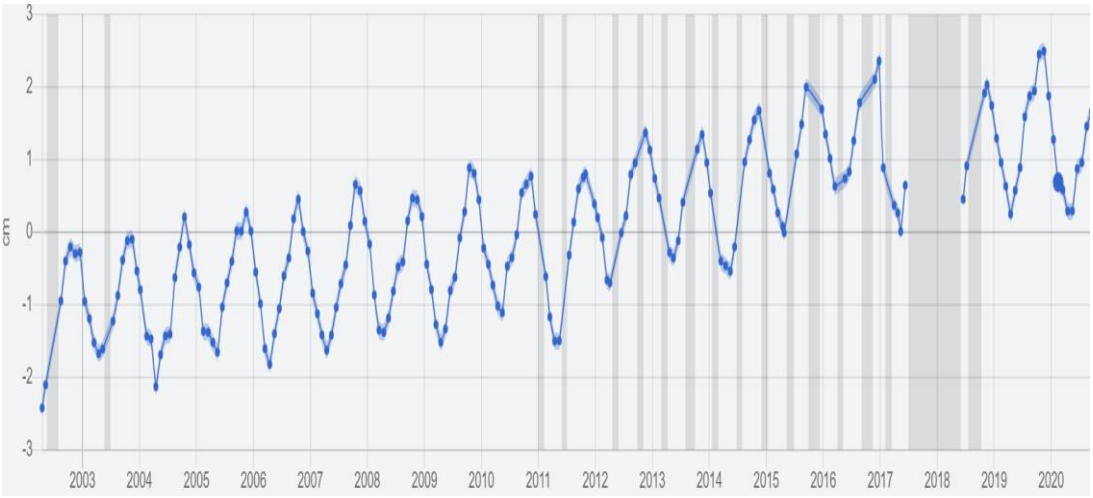

Figure 3.4 The global ocean bottom pressure variability [51]

Figure 3.4 explains the global time series of seafloor pressure changes obtained by the GRACE satellite from 2002 to 2020. The gaps are shown by grey color which states that the time series need to be interpolated and in the following table are declared. The vertical axis states the height of pressure that enters seawater and declares the thickness of liquid water obtained from the GRACE satellite.

Year	Gaps In the Dataset Through Months
2002	**May, June, July, August**
2003	**May, June**
2010	**December**
2011	**January, June**
2013	**March, August, September**
2014	**February, July, December**
2015	**June, October, November**
2016	**April, September, October**
2017	**February, July to December**
2018	**January to May, August, September**

Table 3.1 Gaps in the GRACE and GRACE-FO dataset

Therefore, the linear trend of the seafloor pressure by fitting a first-order polynomial to evaluate the tendency of this linear trend is estimated, which increases by an annual ratio of .0009. As it is known, for time series, the confidence interval is considered, which the consideration is the 95% confidence interval, that shows if the fluctuations are within and inside this interval, it means that this linear trend is the answer to the work. Then, the time series for the earthquakes that occurred in Japan from 2002 to 2019 is extracted. All the earthquakes that happened could be shown from 2002 to 2019 and the major earthquakes such as the one that happened in 2011 with the magnitude of 9.1Mw could be shown at this time series.

3.3 Apply Continuous Wavelet Transform

The CWTs are used to analyze the spectral content of the time series. CWT is a redundant representation. It is possible to retrieve the signal with sampled CWT. If a = 2^{-m} and b= n2^{-m} then the MRA of the signal can be calculated by the following equations.

$$d_{m,n} = \text{CWT}\ (2^{-m}\ , \text{n}2^{-m}) = 2^{\frac{m}{2}} \int_{m,n} s(t)\, \psi^{*}(2^{mt-n}) dt$$

$$d_{m,n} = \int_{m,n} s(t)\, \psi^{*}(t) dt$$

$$\psi_{\ m,n}\ (t) = 2^{\frac{m}{2}} \psi\ (2^{mt-n})$$

$$s(t) = \sum_{-\infty}^{+\infty} \sum_{-\infty}^{+\infty} d_{m,n} \hat{\psi}_{\ m,n}\ (t) \qquad (3.1)$$

If $\hat{\psi}_{\ m,n}\ (t) = \psi_{\ m,n}\ (t)$

$$s(t) = \sum_{-\infty}^{+\infty} \sum_{-\infty}^{+\infty} d_{m,n} \psi_{\ m,n}\ (t)$$

$$d_{m,n} = \int_{m.n} s(t)\, \psi_{\ m,n}\ (t) dt$$

3.4 Applying Cross-Wavelet Transform

The Cross-wavelet transform (XWT) is a data analysis method for geological time-series introduced by Hudgins [50]. The power and phase relationship between two continuous wavelet transforms can be examined simultaneously. The XWTs as defined in the following condition:

$$C_r WT_{kl}\ (c, d)\ =\ Y_{\ k}\ (c, d)\, Y_{\ l}\ (c, d) \qquad (3.2)$$

where the transforms of two signals $k(t)$ and $l(t)$: $Y_{\text{k}}\,(c, d)$ and $Y_{\text{l}}\,(c, d)$. There are simple ratio and variance metrics that could have been supposed to scrutinize the correlation among the transform components on the transform plane (c, d) for example the XWT of two-time series, a = {an} and b = {bn} is being by the above equation [44]:

$$C_r WT_{kl}(c,d) = \mathrm{w}_{\mathrm{n}}^{\mathrm{ab}} = \mathrm{w}_{\mathrm{n}} \mathrm{a} \mathrm{w}_{\mathrm{n}}^{\mathrm{b}^*} \quad (3.3)$$

3.5 Analyzing Cross-Wavelet Transform

To comprehend the examination of the XWT needs to define the wavelet coherency and phase difference which is declaring the correlation in two-time series [45].

3.5.1 Wavelet Coherency

Wavelet coherence is described as the ratio of the cross-spectrum to the product of the spectra of the individual series and as the local correlation, in both time and frequency, between two-time series, a = {an} and b = {bn}. The S signifies a smoothing operator in both time and scale [44].

$$\mathrm{R}_{\mathrm{n(s)}} = \frac{|S(s^{-1}\, \mathrm{w}_{\mathrm{n}}^{\mathrm{ab}}(\mathrm{s}))|}{s(s^{-1}|\, \mathrm{w}_{\mathrm{n}}^{\mathrm{a}}|)^{\frac{1}{2}}\, s(s^{-1}|\, \mathrm{w}_{\mathrm{n}}^{\mathrm{b}}|)^{\frac{1}{2}}} \quad (3.4)$$

3.5.2 Phase Coherence

The intervals of the alternations among two-time series, x = {xn} and y = {yn}, as a frequency and the phase, is φ which the phase difference, φ(x,y), describes the phase relations among the two-time series.

$$\varphi(\mathrm{x},\mathrm{y}) = tan^{-1}\left(\frac{I\,\{\mathrm{w}_{\mathrm{n}}^{\mathrm{xy}}\}}{R\,\{\mathrm{w}_{\mathrm{n}}^{\mathrm{xy}}\}}\right) \qquad \text{with } \varphi(\mathrm{x},\mathrm{y}) \in (\pi, -\pi) \quad (3.5)$$

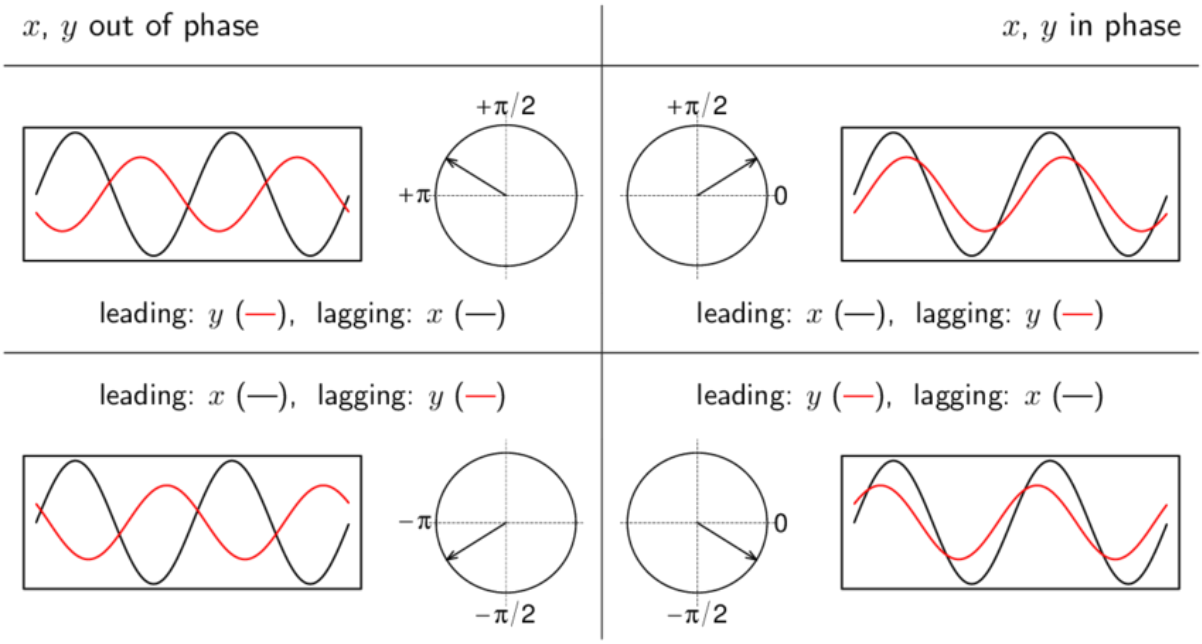

Figure 3.5 Definition of phase differences [52]

If φ(x, y) ∈ (0, π/2) then the series moves in part, however, the x is prior to y. If φ(x,y) ∈ (− π/2, 0) then x is ahead. If φ(x,y) ∈ (π, −π) designates an out-of-phase relationship. If φ(x,y) ∈ (π/2, π) then x is prominent. The y is prominent if φ(x,y) ∈ (−π, − π/2).

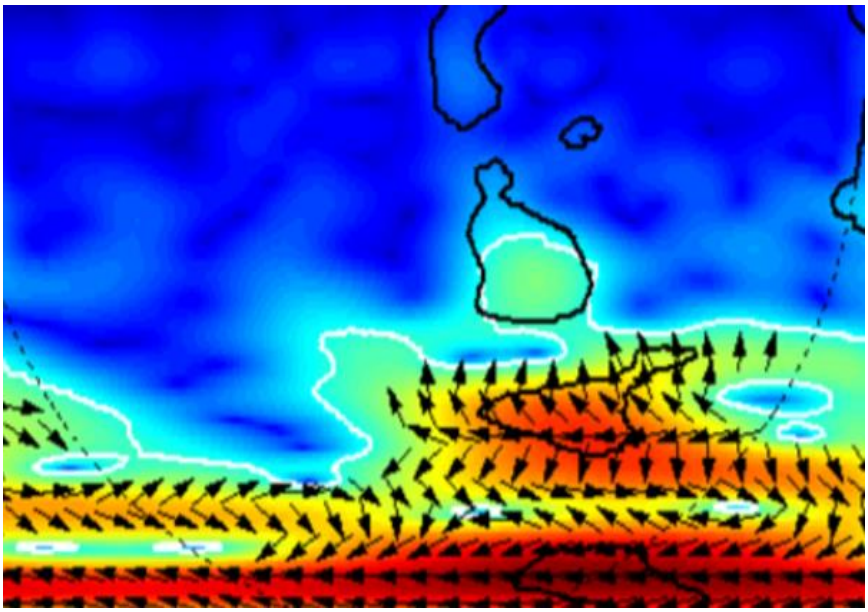

Figure 3.6 An example of cross-wavelet transform [52]

Figure 3.6 presents an example of phase difference which is defined by the Monte Carlo simulations; the white contour denotes the 5% significant level against a white noise null. The black contour denotes the calculable 5% significant level. The cone of influence, indicating the region full of the edge effects, is presented with a dotted line. Inclusively, the wavelet coherence and phase difference could be supposed of as the local, or time-resolved relation between two-time series which is enlightened by Monte Carlo simulation which is worthwhile that the arrows in the cone of influence illustrate the relations on the grounds that the arrows are in the right direction inform the relation that leading the results of the variables in phase [53, 56].

3.6 Validation of the Results

Studying and evaluating the earthquakes in Japan and applying the CWT in both time series, since these two-time series are not stationary, the XWT is used, which can be

analyzed by observing the phase difference. It is mentioned that the XWT method was used to prove the studies of seismically effects of the December 2004 and March 2005 Sumatra earthquakes in GRACE satellite gravity by using the WT [54]. And the XWT was used to explore the relationship between the sunspot activity cycle and rainfall patterns through 11years in Iran. The CWT is utilized for each time series and then the correlation between them is determined by the XWT. The XWT analyzes the temporal relationship between the cycles of sunspot number and means annual precipitation [6].

The studies on solar activity and major earthquakes in Chile were also carried out using the XWT for the sequences of sunspots and earthquake activity. The earthquakes that occurred in Chile are studied, then the mean total sunspot number is considered to analyze the influence of solar activity on large earthquakes. For both, the time series are extracted and analyzed using the CWT. Then, the XWT is used to find the correlation between them, which identifies the 8- to 12-year intonation of the earthquakes [5]. Or studies to analyze infrasound and seismic signals using XWT. Wavelet analysis helps to search for earthquake signatures on the GRACE satellite, which could be utilized to identify the geoid variations given by the December 2004 (Mw = 9.2) and March 2005 (Mw = 8.7) Sumatra earthquakes. Two characteristic time scales for the relaxation were found, with a rapid change occurring near the central Andaman Ridge [4]. In this study, the confidence regions in the XWT figure will be used to discuss the identified relationships among the seafloor pressure and earthquake occurrence.

4 RESULTS

In this section, application and results will be scheduled for the methodology defined before. First, the groundwork of the dataset is listed. The results of extracting the time series of both datasets are demonstrated with supplementary figures. The visual evaluation of the continuous wavelet transform for each time series is listed and utilizing the cross-wavelet transform is listed and analyzed with a phase difference. The results reviewed from the study are discussed.

4.1 Utilization of Data

First, the time series of seafloor pressure which is obtained from GRACE and GRACE-FO measurements were analyzed from 2002 to 2019, then Japan in the account of its territory is selected that is significant to us and needs to be mentioned as earthquakes-prone areas and its four sides are covered with water. Afterward, the same time series of the earthquakes that happen in Japan from 2002 to 2019 be analyzed that help in focusing on the earthquake that happen in 2011.

4.2 Extracting the Time Series

The datasets taken from the GRACE satellite are analyzed; the results are seen in Figure 4.1. It shows that some of the datasets are missing, which makes it difficult to intercept, in order to get a uniform time series, it needs to be interpolated. It is better to point out that LWE is the density that measures from GRACE satellite to the density of the water, and it is a combination of the pressure of the weight of the seawater and the atmosphere above it that consider the seafloor pressure which the units of LWE is Kg/m^3 and if the height of the water is considered the units is being cm or mm.

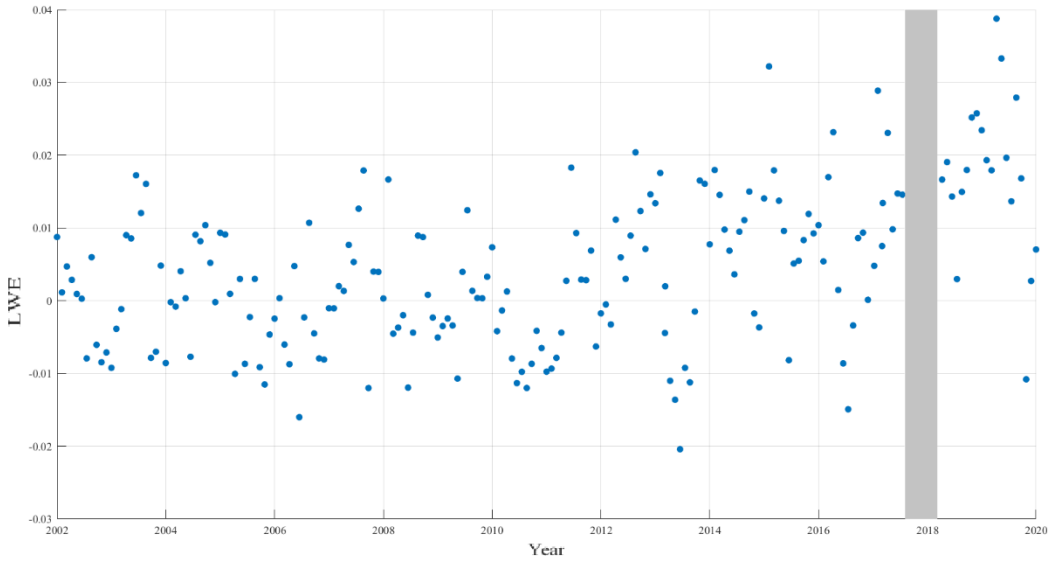

Figure 4.1 Extracted Time Series of averages over Japan

The extracted time series over Japan is displayed in Figure 4.1 between 2002 to 2020, and the grey part illustrates the missing data through the GRACE and GRACE-FO between October 2017 to May 2018. The gaps in the datasets need to be interpolated through the averaged values in datasets. Thus, the interpolation through the averaged values obtained from the GRACE satellite in the MATLAB environment is done. The values averaged over Japan are displayed in the time series in Figure 4.2.

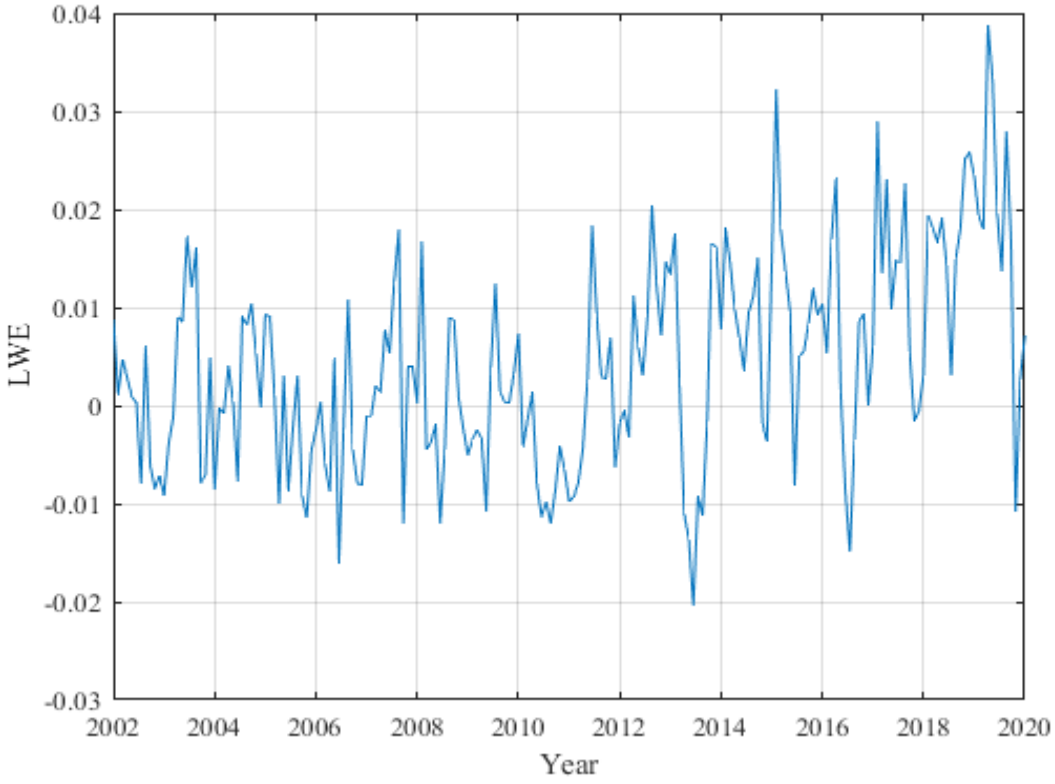

Figure 4.2 Time series of seafloor pressure between 2002 and 2019

Figure 4.2. illustrates the time series of seafloor pressure from 2002 to 2019. Seafloor pressure has been a steady trend until 2010, after which there is a drop (minimum) between 2013 and 2014. There is a slightly increasing trend after 2011 and the pattern before 2011 does not continue.

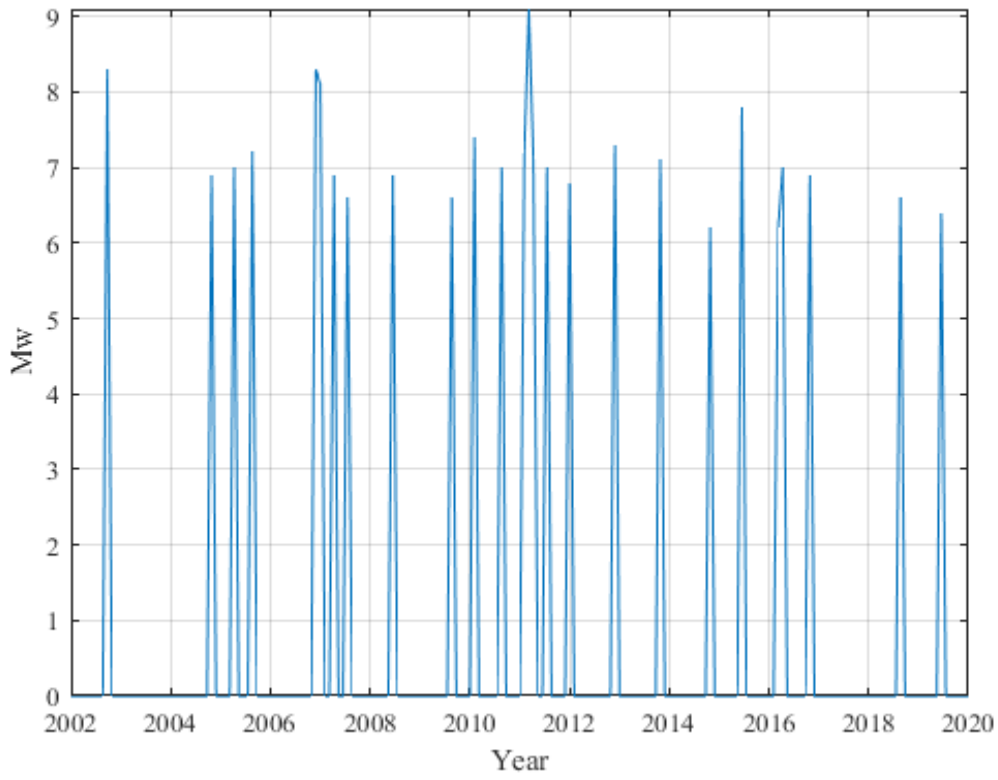

Figure 4.3 Time series of earthquakes larger than 6Mw between 2002 and 2019

Figure 4.3 illustrates the earthquakes larger than 6 Mw from 2002 to 2019. According to the time series, magnitudes fluctuate between 6Mw and 8Mw.

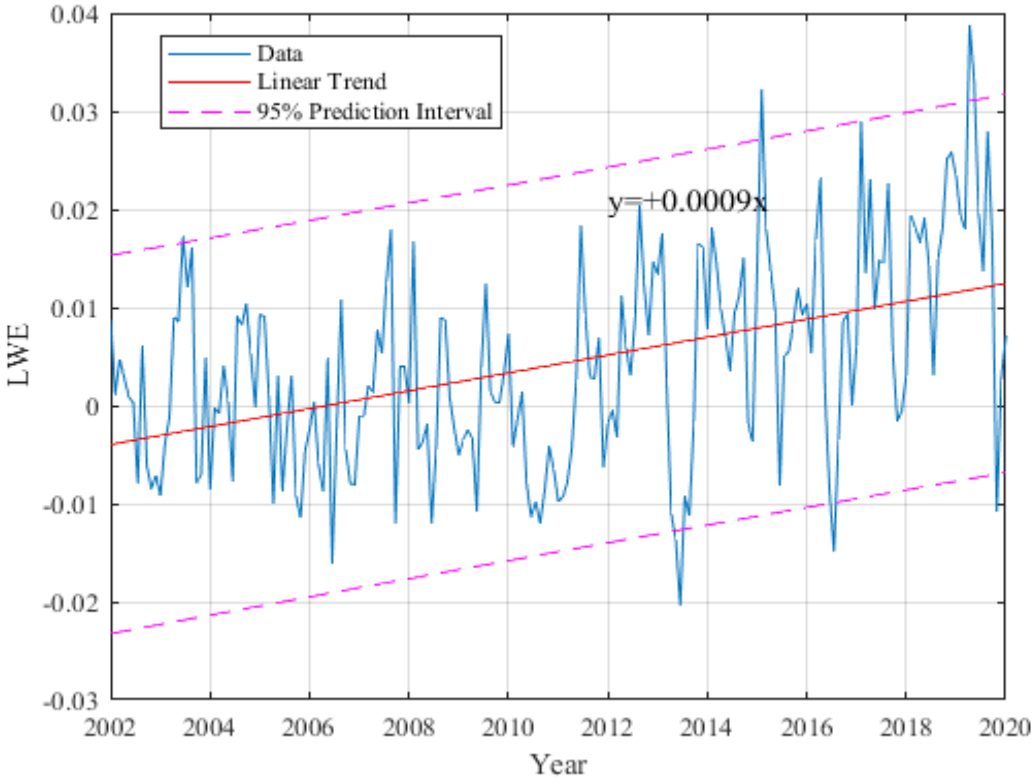

Figure 4.4 Linear trend in seafloor pressure with 95% confidence interval

In the next step, the linear trend of seafloor pressure was estimated to be about 0.0009 annually. The linear trend of the estimated seafloor pressure along with the 95% confidence level is shown in Figure 4.4 which is illustrated that there might be a relationship between the fluctuations that increased after the earthquake that happen in 2011.

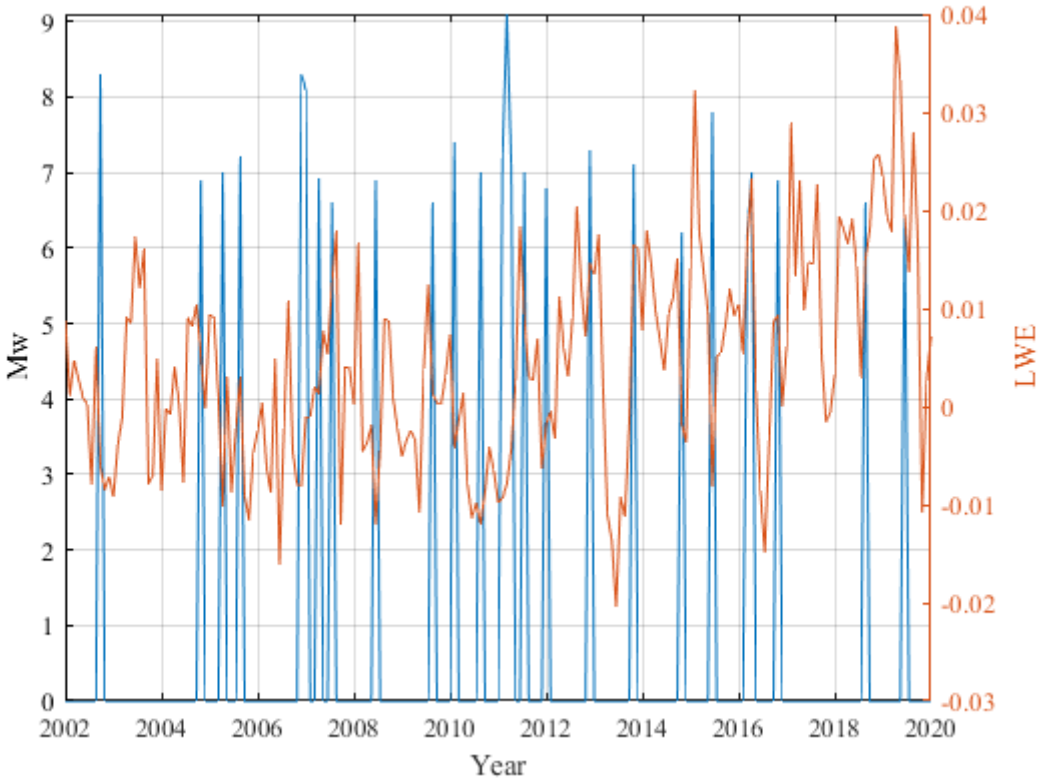

Figure 4.5 Comparing two-time series that have been extracted

While comparing the two-time series as shown in Figure 4.5, the seafloor pressure has increased after the 2011 earthquake, which might indicate that the seafloor pressure has been affected by the earthquake.

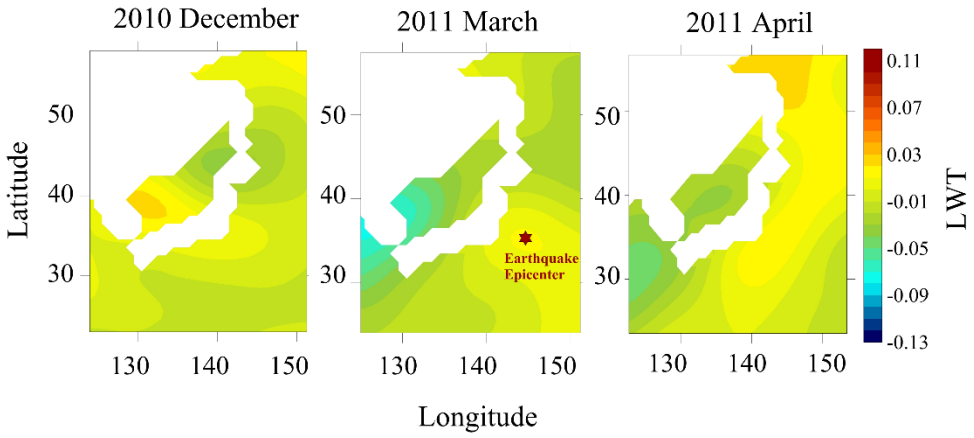

Figure 4.6 Japan's spatial and temporal map of seafloor pressure changes

To better understand whether the seafloor pressure has increased after the 2011 earthquake, we examine the spatial and temporal map of Japan for seafloor pressure changes before and after the earthquake occurrence through the MATLAB environment, which shows that the seafloor pressure after the earthquake has changed and increased in some parts.

4.3 Applying Continuous Wavelet Transform

In the next step, CWT is utilized to identify the periods of each time series. The data is of non-stationary nature which warrants wavelet transformation to process the data. After analyzing each time series with the CWT, the correlation between the two-time series is analyzed by XWT.

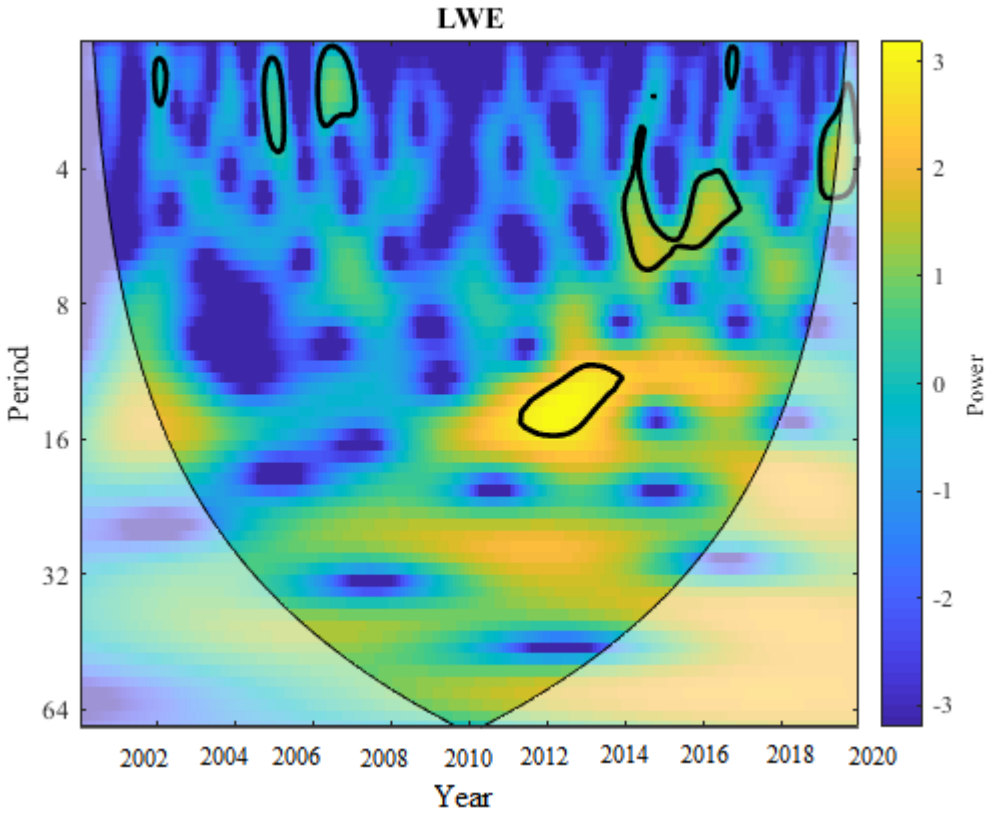

Figure 4.7 CWT of seafloor pressure time series

Figure 4.7 shows the CWT of the seafloor pressure time series, in which the vertical axes show the periods based on monthly and colors of spectral power. The bright blue color designates low spectral power and the bright yellow color indicates high spectral power where we focus on highlighting high spectral power. A thick black contour designates a 5% significance for red noise separation and impact cone (cone of influence).

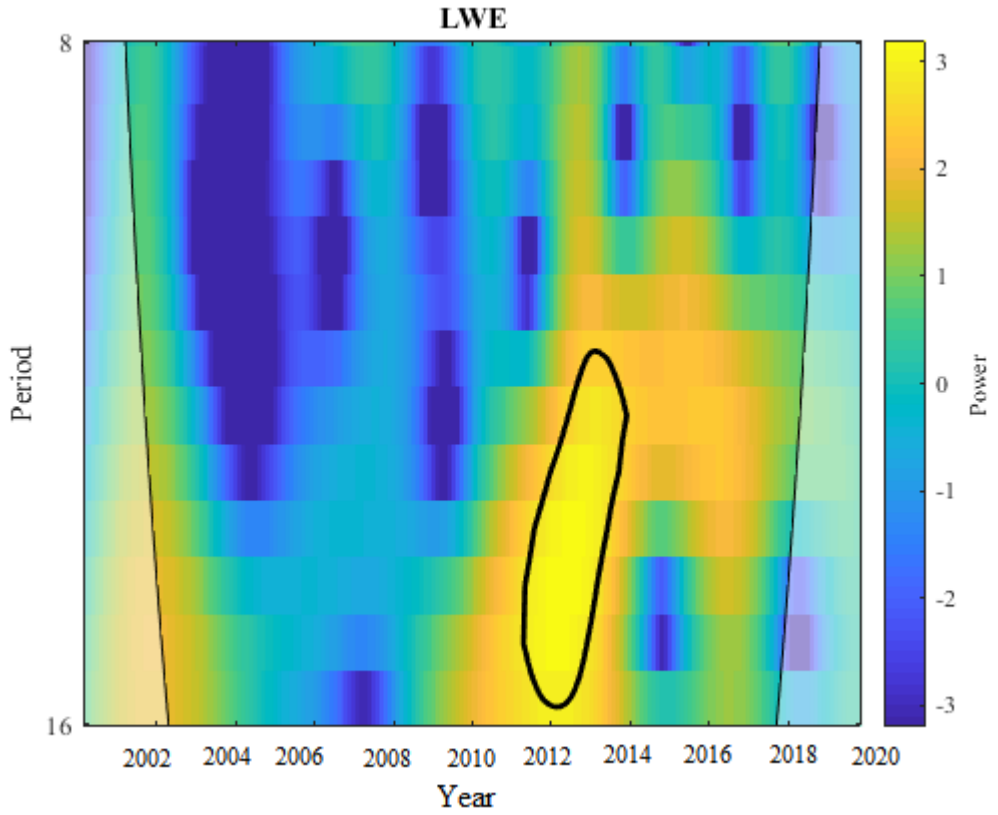

Figure 4.8 Periods of 10 to 16 months of seafloor pressure between 2010 and 2014

In periods of 10 to 16 months, the seafloor pressure between 2010 and 2014 is high, as shown in Figure 4.8.

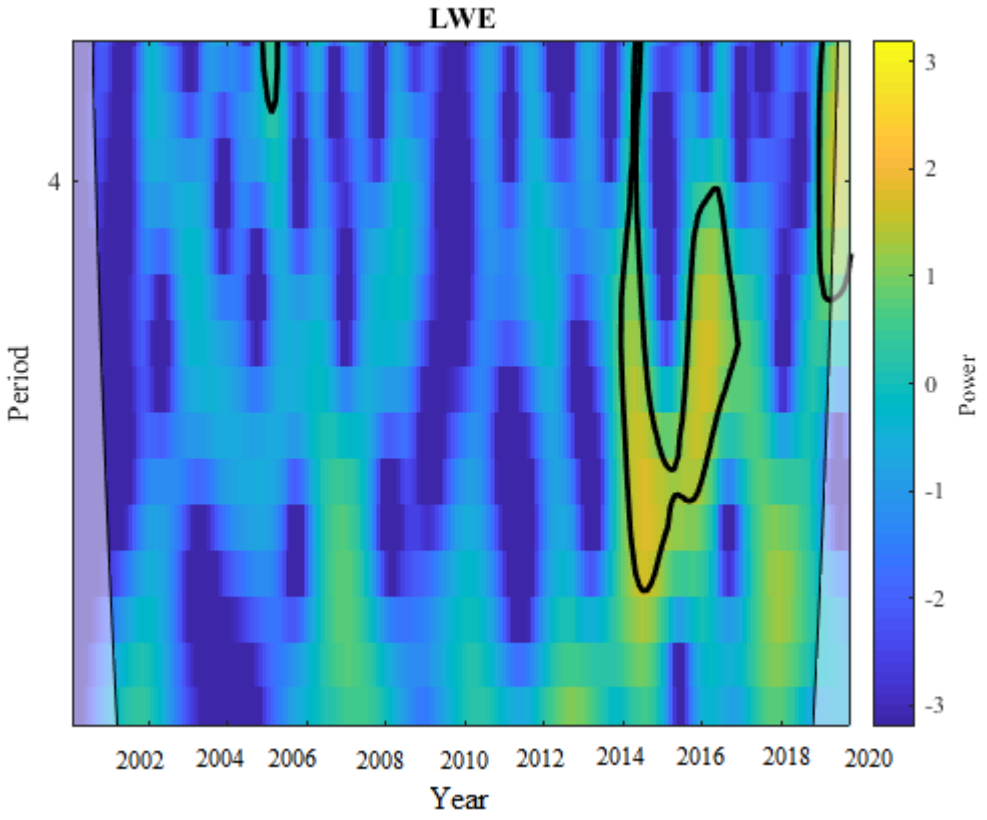

Figure 4.9 6-Month period of seafloor pressure between 2014 and 2017

In the 6-month periods, the seafloor pressure between 2014 and 2017 shows high strength, which is shown in Figure 4.9.

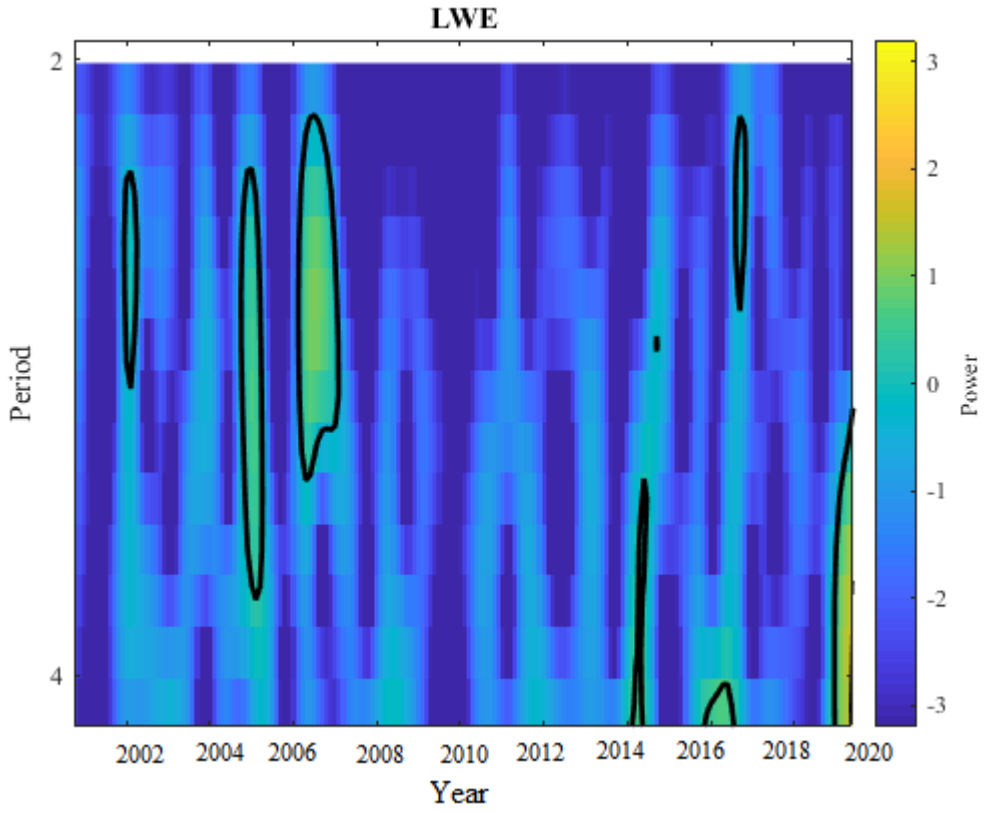

Figure 4.10 3-Month seafloor pressure periods between 2005 and 2007

In the 3-month periods, the seafloor pressure between 2005 and 2007 is high, as shown in Figure 4.10.

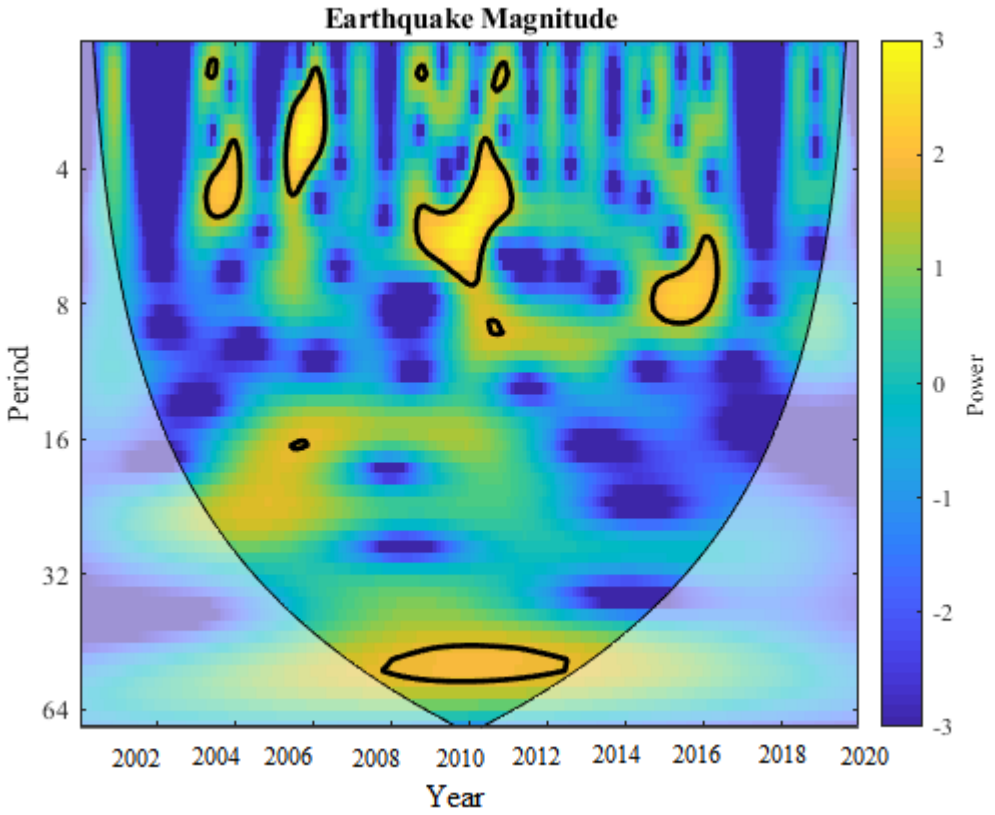

Figure 4.11 The CWT of earthquake time series

Figure 4.11. shows the CWT of large earthquake time series, in which the vertical axes show the periods based on monthly and colors of spectral power. The bright blue color indicates low spectral power and the bright yellow color indicates high spectral power that is looking to discover high spectral power. The thick black contour of the circle indicates the importance of 5% for the separation of red noise and impact cone.

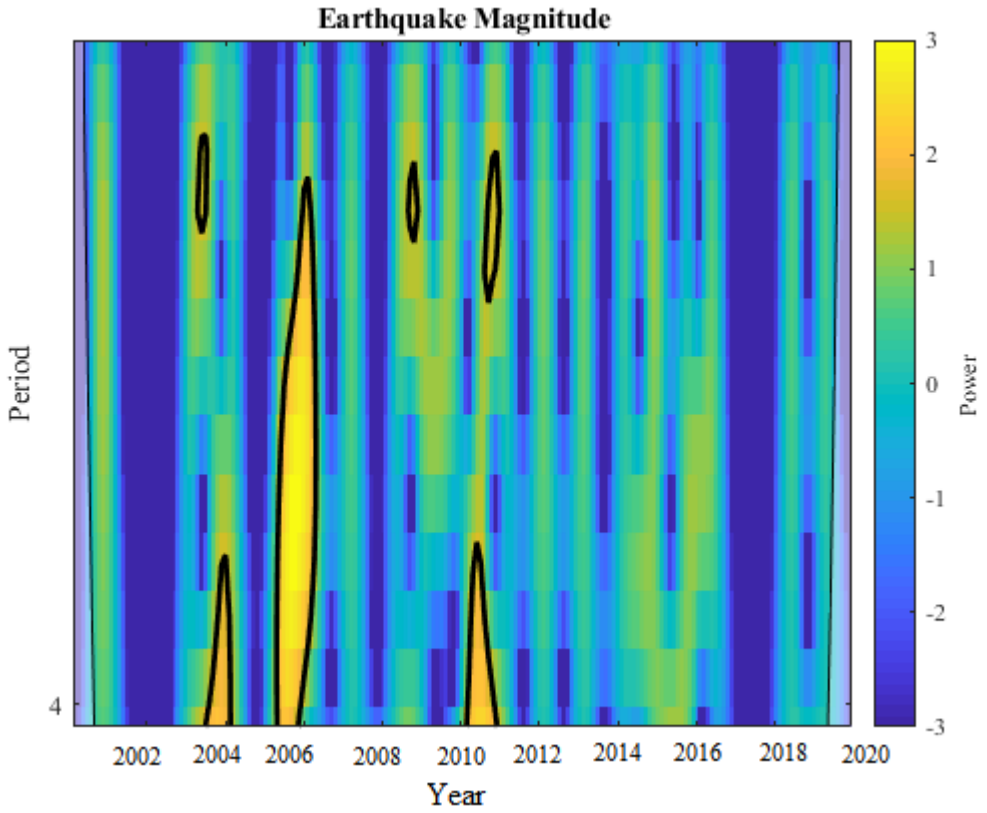

Figure 4.12 3-Month periods of earthquakes between 2005 and 2007

High magnitude earthquakes during the three-month period between 2004 and 2006 are shown in Figure 4.12.

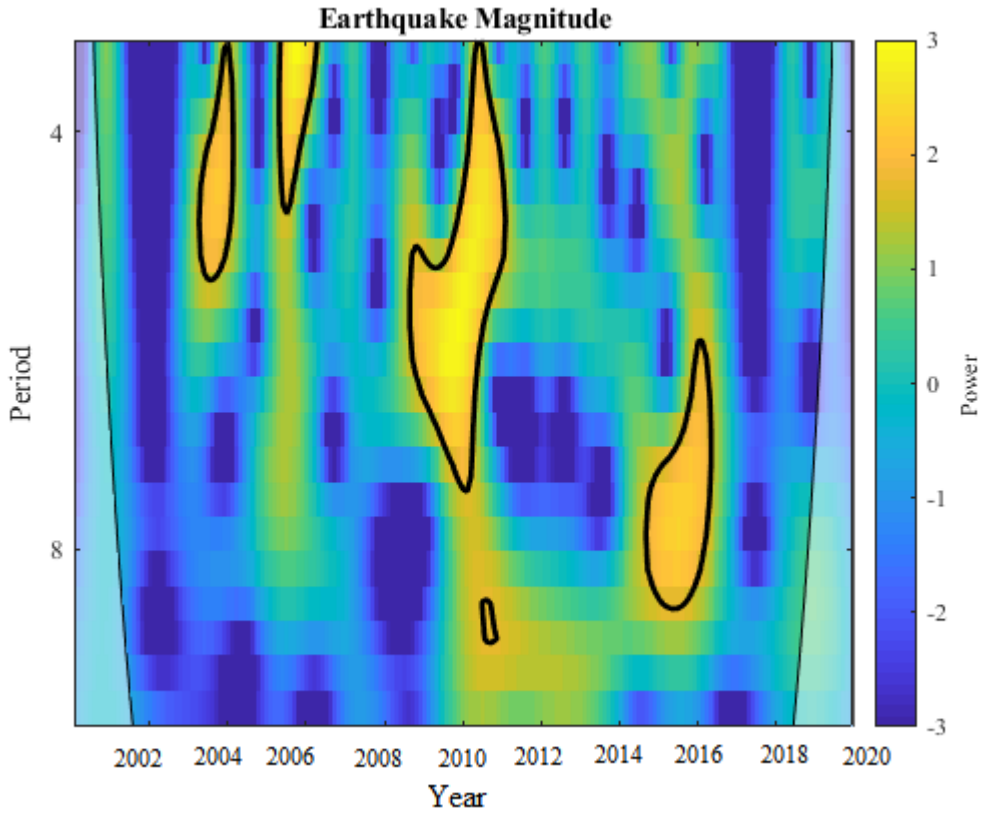

Figure 4.13 6-Month and 8-Month periods of major earthquakes between 2014 and 2017

High magnitude earthquakes during the six-month period between 2008 and 2010 are shown in Figure 4.13. High magnitude earthquakes are observed during the large 8-month periods between 2015 and 2016.

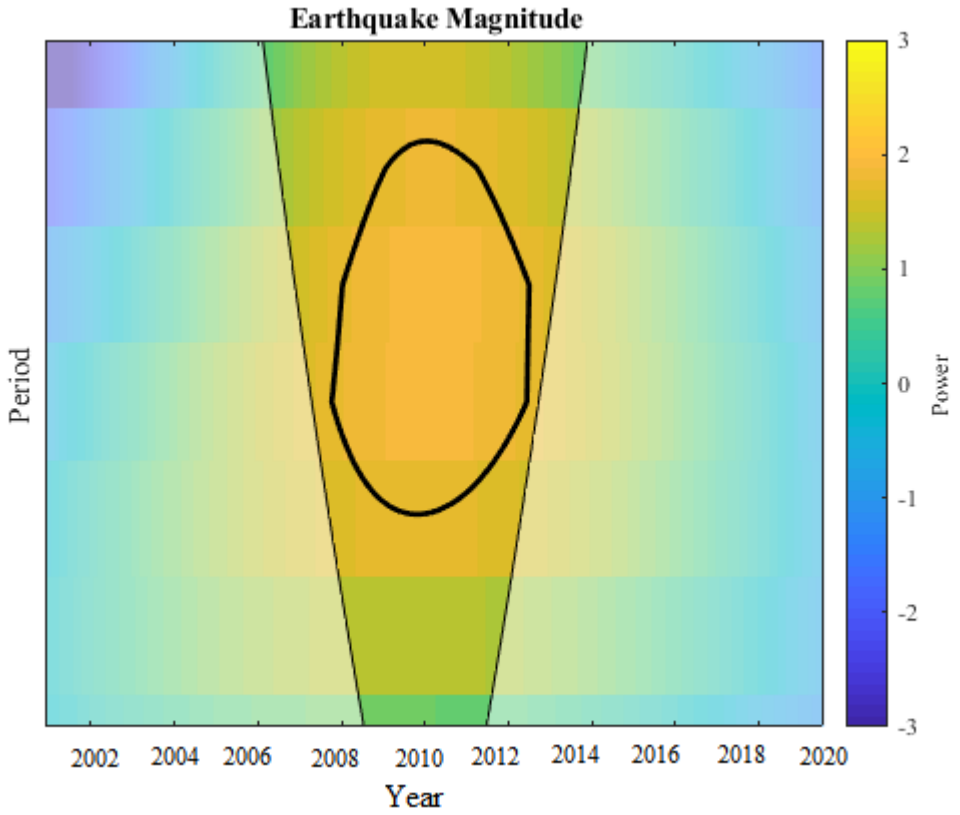

Figure 4.14 60-Month periods of major earthquakes between 2009 and 2012

During the periods of about 60 months of the great earthquake between 2009 and 2012, high strength is observed, which is shown in Figure 4.14.

4.4 Applying Cross-Wavelet Transform

In the next step, XWT is used to analyze the two-time series and the results are analyzed.

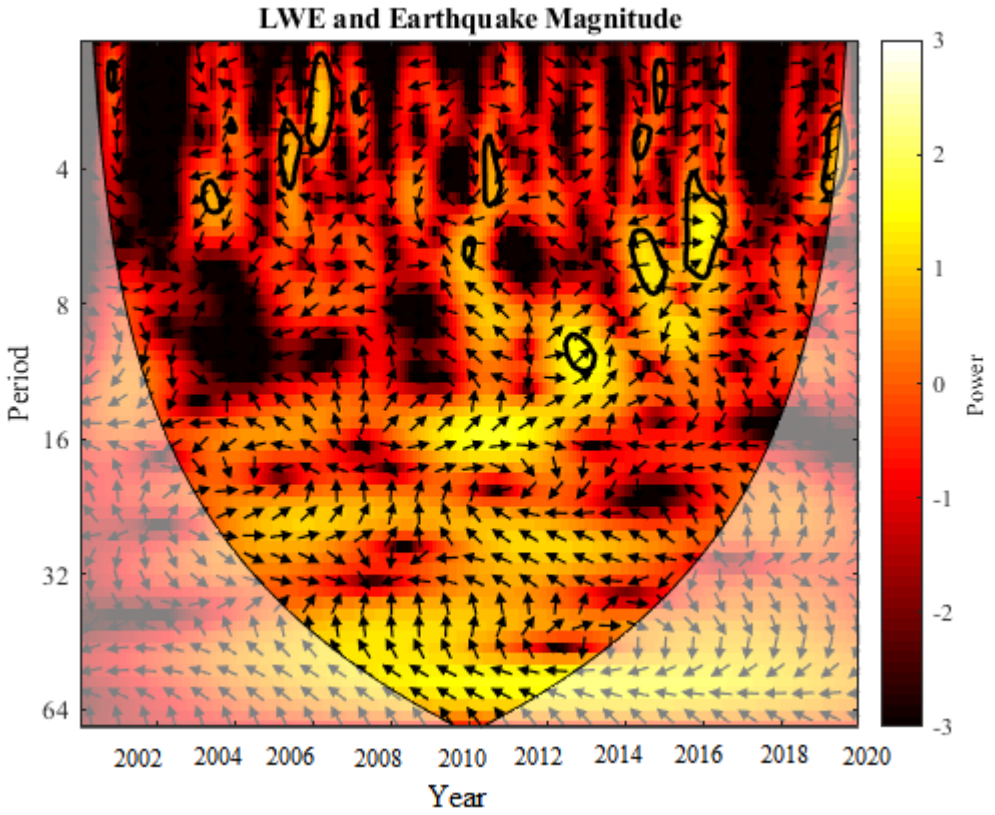

Figure 4.15 Cross-Wavelet transform of ocean bottom pressure and earthquakes

Figure 4.15 displays the XWT of the seafloor pressure and the magnitude of the earthquake. The crimson color indicates low spectral power and the bright white color indicates high spectral power, where high spectral power indicates both signals have common power in the same time with similar periods. The thick black contour of the circle indicates the importance of 5% for the separation of red noise and impact cone.

4.5 Analyzing Cross-Wavelet Transform

The relation of the relative phase to the arrow is shown; arrows in the right direction illustrate the same phase, to the left direction presents the opposite phase, other directions may be read as the lag between the seafloor pressure signal by the magnitude of the earthquake.

In the years 2006 to 2010, high power and periods of about 6 months are observed, in which the arrows are mainly upwards, i.e., the leading of the magnitude signal of the earthquake by the pressure signal. From 2009 to 2011, high power and 12-month periods are observed, with the arrows mostly to the right, meaning that the two signals of the seafloor pressure and the magnitude of the earthquake are in phase. From 2012 to 2014, high power and 10-month periods are observed in which the arrows are mainly to the right, meaning that the two signals of the seafloor pressure and the magnitude of the earthquake are in phase. From 2014 to 2016, high power and 6-month periods are observed in which the arrows are mainly to the right, i.e., the two signals of the seafloor pressure and the magnitude of the earthquake are in phase.

4.6 Discussion

The main goal of this study is to study whether the dataset obtained from the GRACE satellite could show the changes by the seafloor pressure that might have relationships with the earthquakes, especially the earthquake in 2011. Based on the methods implemented in this study, first of all, creating a time series for the seafloor pressure data, fitting the first-order line to evaluate the tendency of this linear trend which shows that the fluctuations of LWE change after 2011. Afterward, the time series of earthquakes larger than 6 Mw from 2002 to 2019 is analyzed to better comprehend an earthquake with

a magnitude of 9.1 Mw in 2011. The linear trend of the seafloor pressure by fitting a first-order polynomial is estimated to measure the tendency of this linear trend which increases by an annual ratio of .0009.

As it is known, for time series, the 95% confidence interval is considered, if the fluctuations are within the upper and lower bound. The WT for non-stationary time series in which fluctuations are average and its standard deviation changes with time, like the time series, are utilized. The periods in time and frequency are revealed, converting the time series of the seafloor pressure into a wavelet domain, which gives a graph that shows the pressure of the samples in the periods and the spectral power. The high spectral power means that if the CWT presents in yellow color, which is obvious that the high spectral power in the 12-month period, which by zooming in on, for example, in 2010 to 2016 high spectral power is shown too. A significant point to note is that the continuous WT analyzes and marks a part inside a thick black contour. The thick contour is the 5% significance that is thrown inside the contour, which means that these are significant signals.

In the next step, examining the large time series of the earthquakes, which are again seen to reveal the thick contours of the earthquakes. After analyzing the worthwhile case, although not marked as significant a very large period related to the 2011 Japan earthquake is seen. The XWT takes two-time series of CWT and tells where these two-time series are related, as shown in Figure 4.15. In analyzing the cone of influence in XWT, a series of arrows represent the relation between two-time series, which indicates the direction of co-movement between variables. If the arrows are in the right direction, it means that time series are in coherence, arrows in the left direction indicate out of phase variables, arrows in the right-up and left-down direction indicate lagging of the variables, and arrows in the left-up and right-down direction indicate leading of the variables. First of all, the arrows display phase differences between the time series. If the angle between

arrows and the x-axis is in $(-\pi/2,0) \cup (\pi/2, \pi)$ then y(t) leading x(t), whereas it is in $(0, \pi/2) \cup (-\pi, -\pi/2)$ then x(t) is leading y(t).

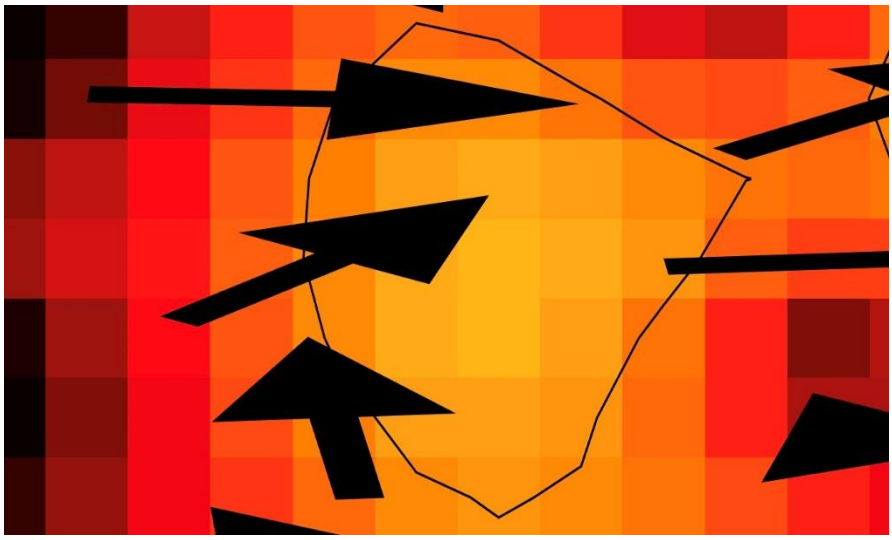

Figure 4.16 Co-Phase of earthquake magnitude and seafloor pressure in 2006

In Figure 4.16, the correlation between seafloor pressure and earthquakes in the 6-month period in 2006 is shown where the seafloor pressure signals with earthquakes in Japan are in phase.

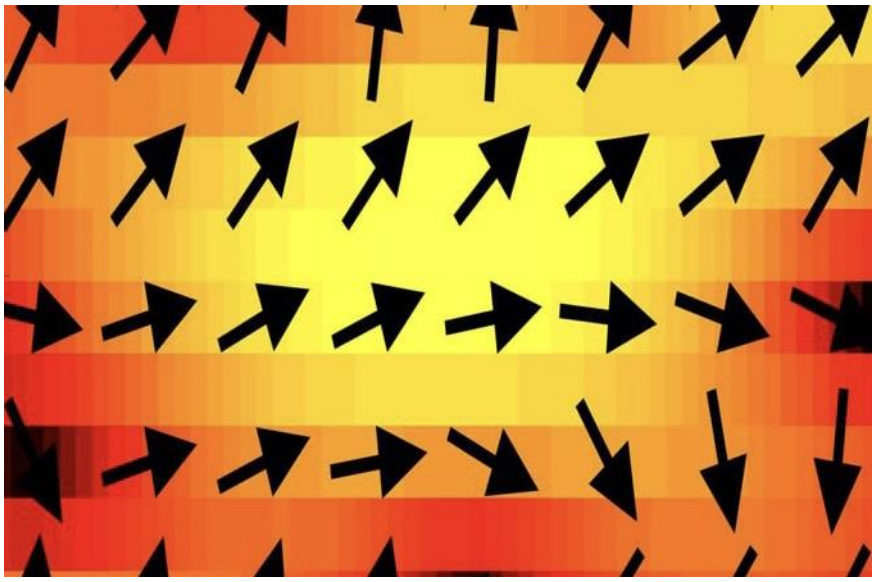

Figure 4.17 Co-Phase of earthquake magnitude and seafloor pressure in 2011

In Figure 4.17, the relationship between seafloor pressure and earthquakes in the 12-month period in 2011 is shown. The arrows are aligned to the right, indicating the phase angle is small or the signals are coherent.

Figure 4.18 Co-Phase of earthquake magnitude and seafloor pressure in 2016

In Figure 4.18 the relationship between seafloor pressure and earthquakes in the 6-month period in 2016 is shown. In this case similar to the previous cases the signals are coherent.

Consequently, Figure 4.16, 4.17, and 4.18 shows the co-phase of the magnitude of the earthquake and the seafloor pressure, which means variations in seafloor pressure which could obtain from the GRACE satellite show a coherent relationship with the earthquakes. This could show that their occurrence and frequency are related to the 2006, 2011, 2016 major earthquakes in Japan. Further investigations are required to analyze the sensitivity of the XWT to the noise content and levels in the signals where the GRACE data has been obtained by Spatio-temporal averaging.

5 CONCLUSION

This study aims to investigate potential relationships between seafloor pressure changes and major earthquakes. The research focuses on the Japan region since major earthquakes occur frequently in the region. The Liquid Water Equivalent Thickness time series acquired by the GRACE satellite is used to represent seafloor pressure changes over Japan from 2002 and 2019. Major earthquakes with moment magnitudes larger than 6 Mw are also compiled into a time series. The relationship between these two-time series is analyzed by the cross-wavelet transform. The analysis of phase coherence in the cross-wavelet transforms shows that there may be a relationship between the seafloor pressure changes recorded by the GRACE satellites, especially around 2011 and 2012. Although the analysis cannot significantly state the causal relationship between both phenomena, it is shown that seafloor pressure data from GRACE may be considered as an additional data source for the study of the coupling between seafloor pressure changes and major earthquakes. Earthquakes are difficult to predict by conventional methods. Identifying the relationship of the earthquakes with other physical phenomena for which observations can be obtained continuously and easily may provide new tools to understand and predict the major earthquakes. The analysis techniques in this study may be repeated for other active regions of the world in order to increase the empirical evidence and knowledge on the possible relationships, where ground-based measurements can also be included. In addition, further investigation on the sensitivity analysis of cross wavelet transform may provide additional insight into the usability of GRACE data.

REFERENCES

1. Balmino, Georges, et al. "CHAMP, GRACE and GOCE: mission concepts and simulations." Applicata 40.3-4 (**1999**): 309-319.
2. S. H. Han, J. Sauber, S. B. Luthcke, C.Ji, and F. F. Pollitz, "Implications of post seismic gravity change following the great **2004** Sumatra-Andaman earthquake from the regional harmonic analysis of GRACE intersatellite tracking data", Geophysical Research,111, B11413, 13, November **2008**.
3. Bao, L. F., A. Piatanesi, Y. Lu, H. T. Hsu, and X. H. Zhou, "Sumatra tsunami affects observations by GRACE satellites", Eos Trans. AGU, (**2005),** 86(39), 353.
4. Panet, Isabelle, et al. "Coseismic and post-seismic signatures of the Sumatra 2004 December and 2005 March earthquakes in GRACE satellite gravity." *Geophysical Journal International* 171.1 (2007): 177-190.
5. Larocca, P.A. (2016) Application of the Cross Wavelet Transform to Solar Activity and Major Earthquakes Occurred in Chile. International Journal of Geosciences, 7, 1310-1317.
6. Nazari-Sharabian, Mohammad & Karakouzian, Moses. (2020). Relationship between Sunspot Numbers and Mean Annual Precipitation: Application of Cross-Wavelet Transform-A Case Study. J. 3. 10.3390/j3010007.
7. Sandau, Rainer. "Status and trends of small satellite missions for Earth observation." *Acta Astronautica* 66.1-2 (2010): 1-12.
8. Fu, Lee-Lueng, et al. "TOPEX/POSEIDON mission overview." (1994): 24369-24381.
9. https://directory.eoportal.org/web/eoportal/satellite-missions/c-missions/champ (Last Access: **01.01.2022**).

10. Ch. Reigber, R. Casper, W. Päffgen, “The CHAMP Geopotential Mission,” IAA 2nd International Symposium on Small Satellites for Earth Observation, Berlin, April 12-16, **1999**, pp. 25-28
11. Reigber, Ch, Hermann Lühr, and P. Schwintzer. "CHAMP mission status." *Advances in space research* 30.2 (2002): 129-134.
12. Tapley, B. D., and Ch Reigber. "The GRACE mission: status and future plans." *AGU Fall Meeting Abstracts*. Vol. 2001. 2001.
13. https://www.esa.int/Applications/Observing_the_Earth/GOCE/GOCE_completes_its_mission (Last Access: **01.01.2022**).
14. Drinkwater, Mark R., et al. "The GOCE gravity mission: ESA’s first core Earth explorer." *Proceedings of the 3rd international GOCE user workshop*. Noordwijk, The Netherlands: European Space Agency, 2006.
15. Balmino G. and Perosanz F., Comparison of geopotential recovery capabilities of some future satellite missions. Proc. IAG Symposium, Gravity and Geoid, Graz, k1994, pp. 403-412
16. Jia, Yingzhuo, et al. "The scientific objectives and payloads of Chang’E− 4 mission." *Planetary and Space Science* 162 (2018): 207-215.
17. variable gravity from GRACE, Time. "Temporal gravity field solutions at the AIUB."
18. Bruinsma, Sean L., et al. "The new ESA satellite-only gravity field model via the direct approach." *Geophysical Research Letters* 40.14 (2013): 3607-3612.
19. Albertella, Alberta, et al. "High resolution dynamic ocean topography in the Southern Ocean from GOCE." *Geophysical Journal International* 190.2 (2012): 922-930.
20. Pavlis, Nikolaos K., et al. "The development and evaluation of the Earth Gravitational Model 2008 (EGM2008)." *Journal of geophysical research: solid earth* 117.B4 (2012).

21. Karpik, A. P., et al. "Analyzing spectral characteristics of the global earth gravity field models obtained from the CHAMP, GRACE and GOCE space missions." *Gyroscopy and Navigation* 6.2 (2015): 101-108.
22. https://www.nap.edu/read/12675/chapter/6 (Last Access: **01.01.2022**).
23. Thomas, Alys C., et al. "A GRACE-based water storage deficit approach for hydrological drought characterization." *Geophysical Research Letters* 41.5 (2014): 1537-1545.https://www.epa.gov/sites/default/files/2015-08/documents/mgwc-gwc1.pdf
24. Cazenave, Anny, et al. "Observational requirements for long-term monitoring of the global mean sea level and its components over the altimetry era." *Frontiers in Marine Science* 6 (2019): 582.
25. "International Hydrographic Organization". Archived from the original on 2014-07-24. Retrieved 2013-10-20.
26. Maschke, John. "The International Hydrographic Organization–an effective international regime." *Maritime Studies* 1999.107 (1999): 9-19.
27. Holt, Jason, et al. "The potential impacts of climate change on the hydrography of the northwest European continental shelf." *Progress in Oceanography* 86.3-4 (2010): 361-379.
28. Andersen, Ole Baltazar, et al. "Improving the coastal mean dynamic topography by geodetic combination of tide gauge and satellite altimetry." *Marine Geodesy* 41.6 (2018): 517-545.
29. Romano, Michele, et al. "Artificial neural network for tsunami forecasting." *Journal of Asian Earth Sciences* 36.1 (2009): 29-37.
30. Paris, Raphaël, et al. "Tsunamis as geomorphic crises: lessons from the December 26, 2004 tsunami in Lhok Nga, west Banda Aceh (Sumatra, Indonesia)." *Geomorphology* 104.1-2 (2009): 59-72.
31. Nakahara, Shinji, and Masao Ichikawa. "Mortality in the 2011 tsunami in Japan." *Journal of epidemiology* (2013): JE20120114.

32. Heidarzadeh, Mohammad, et al. "Historical tsunami in the Makran Subduction Zone off the southern coasts of Iran and Pakistan and results of numerical modeling." *Ocean Engineering* 35.8-9 (2008): 774-786.
33. Tendero, Claire, et al. "Atmospheric pressure plasmas: A review." *Spectrochimica Acta Part B: Atomic Spectroscopy* 61.1 (2006): 2-30.
34. https://www.toppr.com/ask/content/concept/measurement-of-atmospheric-pressure-208848/(Last Access: **01.01.2022**).
35. Davis, Lance A., and Robert B. Gordon. "Compression of mercury at high pressure." *The journal of chemical physics* 46.7 (1967): 2650-2660.
36. Smith, Edward H. *A practical method for determining ocean currents*. No. 14. United States Coast Guard, 1926.
37. Bunge, Hans-Peter, et al. "Time scales and heterogeneous structure in geodynamic Earth models." *Science* 280.5360 (1998): 91-95.
38. By Kelvinsong - Own work, CC BY-SA 3.0, https://commons.wikimedia.org/w/index.php?curid=23966175 (Last Access: **01.01.2022**).
39. Sibson, Richard H. "Earthquake faulting as a structural process." *Journal of structural geology* 11.1-2 (1989): 1-14.
40. Chinn, Lisa (25 April 2017). "Earth's Structure From the Crust to the Inner Core". Sciencing. Leaf Group Media. Retrieved 28 June2019.
41. Kanamori, Hiroo (July 10, 1977), "The energy release in great earthquakes", Journal of Geophysical Research, 82 (20): 2981–2987
42. De Boer, Jelle Zeilinga, and Donald Theodore Sanders. *Earthquakes in human history*. Princeton University Press, 2021.
43. Sansom, George Bailey. A History of Japan to 1334. Vol. 1. Stanford University Press, **1958**.
44. Y. Meyer, Wavelets: Algorithms and Applications, SIAM, Philadelphia, 1993
45. Polikar R.; "The wavelet utorial"; htp:/users.rowan.edu/~polikar/WAVELETS, 2006

46. Stanković, Radomir S., and Bogdan J. Falkowski. "The Haar wavelet transform: its status and achievements." Computers & Electrical Engineering 29.1 (2003): 25-44.
47. https://JPL%20TELLUS%20GRACE%20Level-3%20Monthly%20Ocean%20Bottom%20Pressure%20Anomaly%20Release%206.0%20version%2003%20in%20netCDF_ASCII_GeoTIFF%20Formats%20%20%20PO.DAAC%20_%20JPL%20_%20NASA.htm(Last Access: **01.01.2022**).
48. https://www.researchgate.net/publication/45509220_Marine_Biodiversity_in_Japanese_Waters
49. IRIS Earthquake Browser. Available online: https://ds.iris.edu/ieb/index.html (Last Access: 01.01.2022).
50. Hudgins, Lonnie, Carl A. Friehe, and Meinhard E. Mayer. "Wavelet transforms and atmopsheric turbulence." Physical Review Letters 71.20 (1993): 3279.
51. http://gravis.gfz-potsdam.de/ocean (Last Access: 01.01.2022).
52. https://atoc.colorado.edu/research/wavelets/bams_79_01_0061.pdf (Last Access: 01.01.2022).
53. Schmidbauer, Harald & Roesch, Angi. (2018). WaveletComp 1.1: A guided tour through the R package.
54. Reuven Y. Rubinstein and Dirk P. Kroese. 2016. Simulation and the Monte Carlo Method (3rd. ed.). Wiley Publishing.
55. Kutoglu, Hakan & Becek, Kazimierz. (2021). Analysis of Ocean Bottom Pressure Anomalies and Seismic Activities in the MedRidge Zone. Remote Sensing. 13. 1242. 10.3390/rs13071242.
56. A. Grinsted, J. C. Moore, S. Jevrejeva. Application of the cross wavelet transform and wavelet coherence to geophysical time series. Nonlinear Processes in Geophysics, European Geosciences Union (EGU), 2004, 11 (5/6), pp.561-566. ffhal-00302394f.